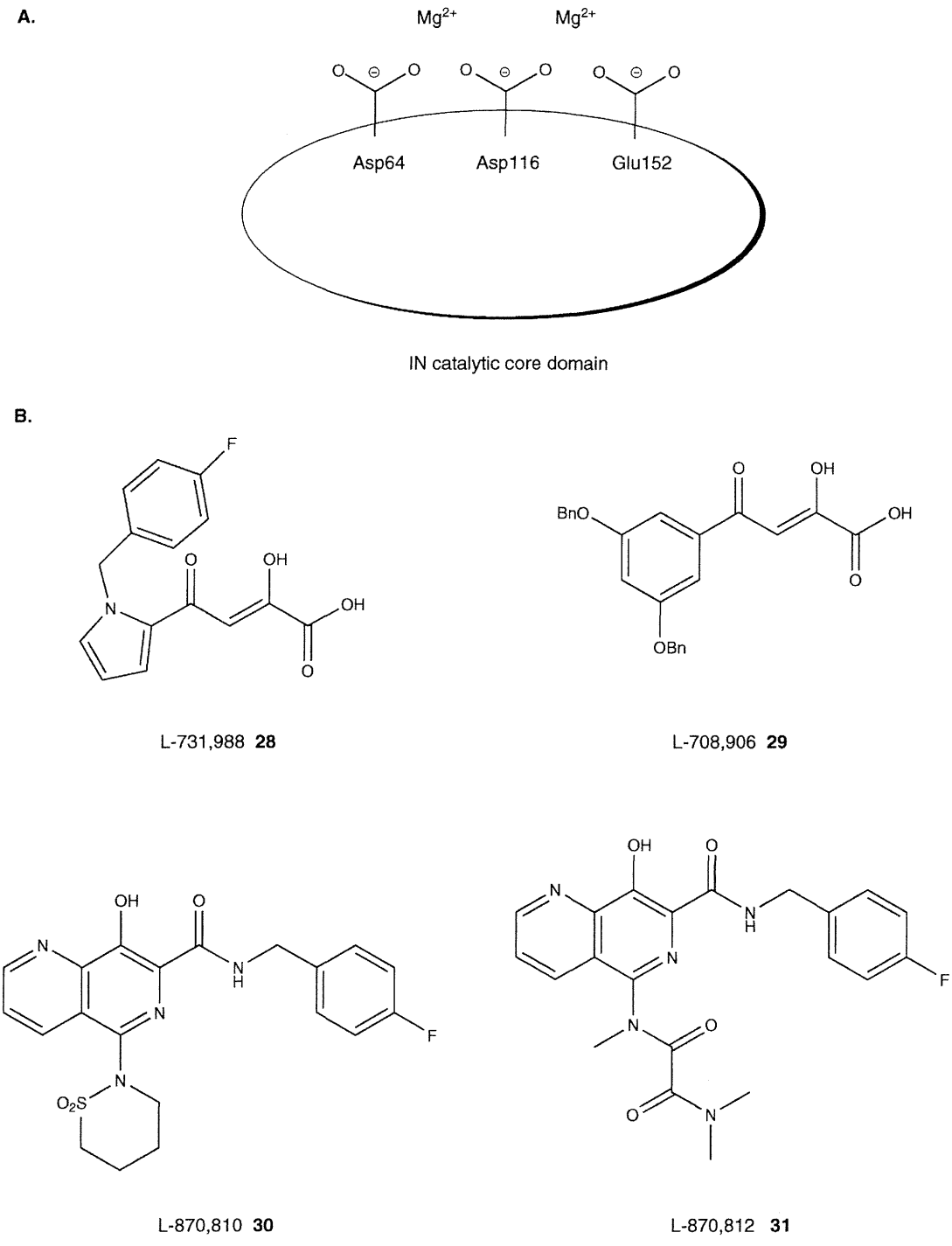

Figure 4. A. Brief presentation of the integrase (IN) catalytic core domain with triad carboxylate residues of Asp64, Asp116 and Glu152, critical for coordination of two magnesium ions. **B.** Structures of DKA type and DKA mimic IN inhibitors. **C.** Structures of naphthyridinone and pyrimidinone-related and other IN inhibitors.

carboxamides, L-870,810 (**30**) and L-870,812 (**31**) (Merck & Co., NJ, USA), have been developed and have shown efficacy in a human and a rhesus simian-human immunodeficiency virus (SHIV) model [77,78]. L-870,810 advanced into the Phase IIa studies and showed viral load reduction, but the trials were terminated due to hepatotoxicity. Subsequent candidate compounds include a naphthyridinone scaffold with a benzyl moiety, such as S/GSK364735 (**32**) (Shionogi-GSK), which has potent anti-HIV activity and HIV-1 RNA reduction activity (**Figure 4C**) [79]. This compound progressed to Phase IIa studies,

C.

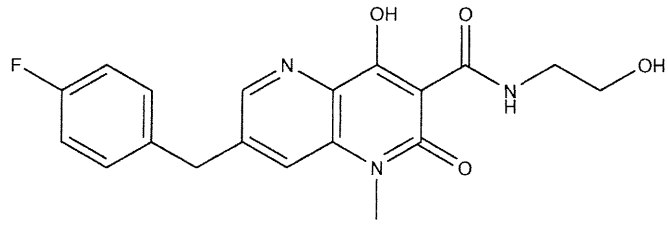

S/GSK364735 **32**

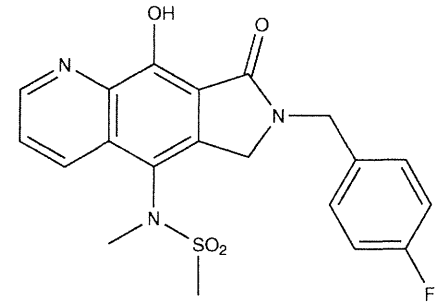

GS-9160 **33**

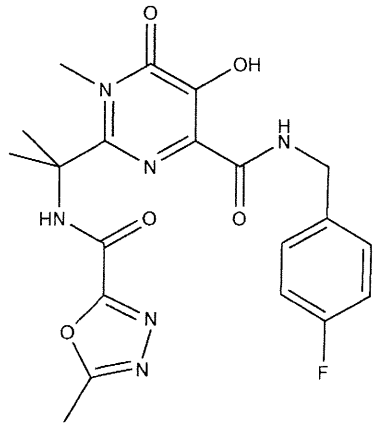

Raltegravir **34**

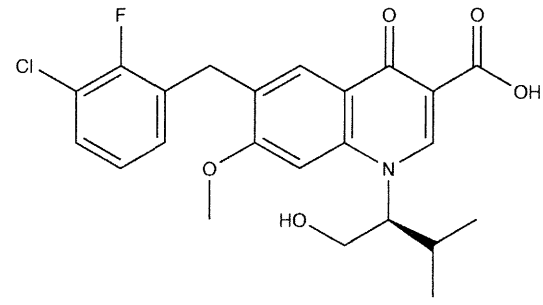

Elvitegravir **35**

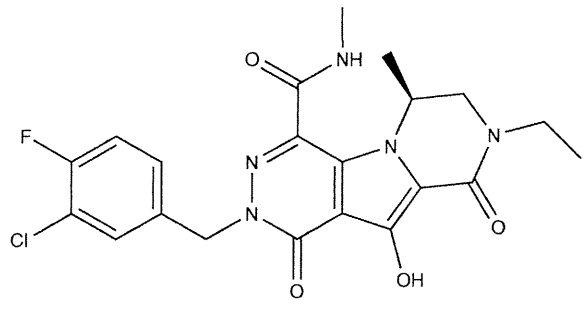

MK-2048 **36**

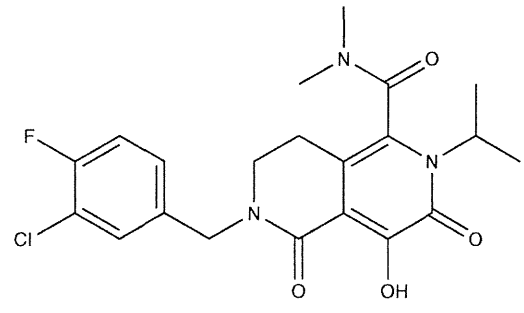

MK-0536 **37**

Figure 4. (continued). A. Brief presentation of the integrase (IN) catalytic core domain with triad carboxylate residues of Asp64, Asp116 and Glu152, critical for coordination of two magnesium ions. **B.** Structures of DKA type and DKA mimic IN inhibitors. **C.** Structures of naphthyridinone and pyrimidinone-related and other IN inhibitors.

but its clinical trial was discontinued due to hepatotoxicity. A tricyclic analog with a quinoline template in combination with a lactam ring and a benzyl moiety, GS-9160 (33) (Gilead Sciences, Inc., Foster, CA, USA), was reported [80]. This compound has a very low EC_{50} and a very high selectivity index of ~ 2000. In addition, it showed synergistic effects in combination with protease inhibitors, NNRTIs and NRTIs. Viral resistance selections with GS-9160 obtained mutations within the catalytic core domain of IN but its pharmacokinetic profile in individuals with once-daily dosing did not achieve antiviral

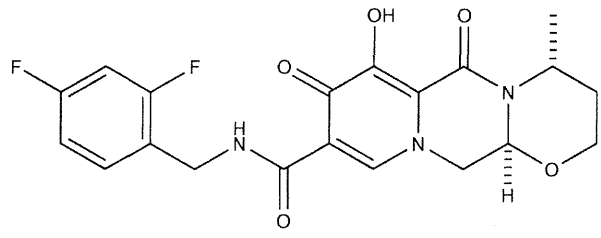

Dolutegravir **38**

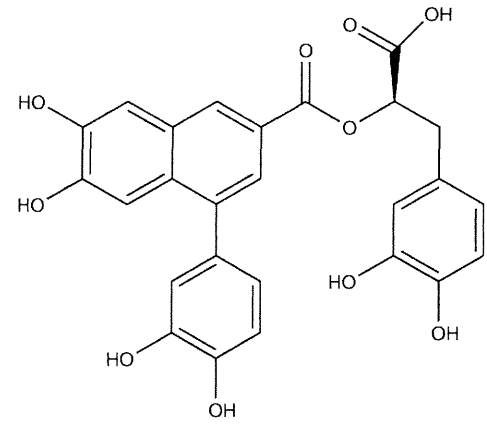

Globoidnan A **39**

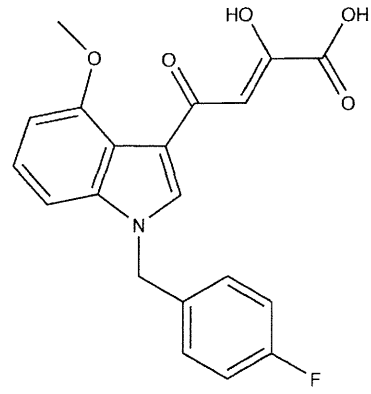

CHI-1043 **40**

Figure 4. (continued). A. Brief presentation of the integrase (IN) catalytic core domain with triad carboxylate residues of Asp64, Asp116 and Glu152, critical for coordination of two magnesium ions. **B.** Structures of DKA type and DKA mimic IN inhibitors. **C.** Structures of naphthyridinone and pyrimidinone-related and other IN inhibitors.

efficacy and the clinical trial of this compound was terminated after Phase I studies.

Raltegravir (34), a pyrimidinone derivative, was the first IN inhibitor to be approved by the FDA [12,13]. This compound has a *p*-fluorobenzyl branch as a common structure and a five-membered heterocyclic ring. In clinical trials, doses of 200, 400 and 600 mg were studied, and the recommended dose of Raltegravir for adults is 400 mg twice a day. In clinical trials patients treated with Raltegravir achieved viral loads of less than 50 copies/ml sooner than those with a dosage of protease inhibitors or NNRTIs. In 2007, Raltegravir was initially approved only for use in patients with resistance to other HAART drugs. However, in 2009, the FDA expanded approval of Raltegravir for use in all patients in combination with other anti-HIV agents. Monotherapy with Raltegravir is unlikely to show durability. Research of effects on latent viral reservoirs and eradication of HIV is in progress. Possible side effects are diarrhea, nausea, headache, fever, rash, Stevens–Johnson syndrome and depression. Concerning emergence of resistant mutants, Raltegravir is likely to lose efficacy due to a major viral mutation compared with protease inhibitors requiring more mutations. A new pyrimido-azepine derivative (PYRAZ) (Merck & Co., NJ, USA), which shows less cross-resistance with Raltegravir-resistant strains, was reported [81]. Elvitegravir (GS-9137/JTK-303) (35) (Gilead Sciences, Inc., Foster, CA, USA/JT, Tokyo, Japan) with a quinolone template also advanced into Phase III studies as the second candidate of IN inhibitors [82]. This compound has nanomolar levels of IN inhibitory and anti-HIV activities together with moderate bioavailability and low clearance. Boosting by a CYP450 inhibitor ritonavir is useful for efficacy of viral load reductions [83]. In addition, another booster agent GS-9350, itself with no antiviral activity, has been tried in a combinational regimen [84]. Elvitegravir showed cross-resistance with Raltegravir-resistant strains [85]. Another potential inhibitor MK-2048 (36) (Merck & Co., NJ, USA) showed

improved potency against mutant strains [86]. Viral mutations in resistance to MK-2048 are different from those with Raltegravir or Elvitegravir. MK-2048 is superior to Raltegravir in terms of retention since it inhibits IN four times longer. Thus, MK-2048 has advanced into Phase III studies. MK-0536 (37) (Merck & Co., NJ, USA) also has a good retention of anti-HIV activity [87]. Dolutegravir (S/GSK1349572) (38) (Shionogi, Osaka, Japan-GSK, Middlesex, UK) is a new generation IN inhibitor with potent anti-HIV activity, a low clearance and good oral bioavailability and which advanced into Phase III trials in February 2011 [88,89]. In evaluation using mutation site-directed mutants, Dolutegravir showed a resistant profile that was different from those of Raltegravir and Elvitegravir, suggesting less cross-resistance with those drugs and a genetic barrier to resistance. Even once-daily monotherapy in humans with Dolutegravir without booster drugs showed efficient reduction in RNA levels, high retention of blood concentrations and good pharmacokinetic profiles. Currently, three-drug combinational use with two NRTIs, Abacavir (ABC) and 3TC, is awaiting approval. Globoidnan A (39), a lignan found in *Eucalyptus globoidea* in Australia, has been found to inhibit the action of HIV-IN [90] but it is not known whether it inhibits other retroviral INs. Since it has a novel structure, this possibility will be investigated further. Future IN inhibitors require a high genetic barrier to resistance, low dose and once-daily dose with good pharmacokinetic profiles in the absence of booster drugs. Structural analysis of the complex of IN and DNA should be useful for the design of new IN inhibitors but structural elucidation of HIV-1 IN has not been succeeded yet in spite of numerous efforts. The crystal structure of human foamy virus IN with viral DNA can be used as an alternative [91,92]. Practically, the binding modes of a new IN inhibitor with a benzylindole derivative, CHI-1043 (40), which has a nanomolar range of inhibitory activity against strand transfer reaction, was analyzed using the above crystal structure of the complex, suggesting that CHI-1043 has the same binding modes as Raltegravir and Elvitegravir [93]. Development of HIV-1 IN inhibitors such as Raltegravir has recently been advanced in AIDS chemotherapy but combinational dosing regimens are necessary because emergence of resistant mutants against Raltegravir has been reported. Investigational drugs such as Elvitegravir and Dolutegravir are anticipated for clinical use.

Recently, we have discovered different types of IN inhibitors [94,95]. By screening a random library of overlapping peptides derived from HIV-1 gene products we have found three Vpr-derived 15-mer peptides with significant IN inhibitory activity, indicating that IN inhibitors exist in the viral preintegration complex (PIC) (**Figure 5A**). These inhibitory peptides are consecutive overlapping peptides. Peptidic 12- and 18-mers from the above original Vpr-sequence with the addition of an octa-arginyl group into the C-terminus to enhance cell membrane permeability have IN inhibitory activity and anti-HIV activity. The detailed mechanism of action of these inhibitors has not been disclosed although it is thought that they may bind to the cleft between the amino-terminal domain and the core domain of HIV-1 IN. This region is distinct from the nucleic acid interacting surfaces, indicating that the Vpr-derived peptides inhibit IN function in an allosteric manner. These data are useful for the development of different types of potent HIV-1 IN inhibitors based on Vpr-derived peptides.

5. CD4 mimics as HIV entry inhibitors

The binding of gp120 to the host-cell surface protein CD4 causes gp120 to undergo a conformational change subsequently binding to the co-receptor CCR5 or CXCR4, as described in Section 1. Thus, CD4-related molecules including soluble CD4 (sCD4) could be inhibitors of HIV entry, although unsuccessful attempts have been made to develop sCD4. Recently, several small CD4 mimics have been found by us and others. These include NBD-556 (41) [96,97], YYA-021 (42) [98-100], JRC-II-191 (43) [101] and BMS806 (44) (**Figure 5B**) [102]. NBD-556, YYA-021 and JRC-II-191 cause a conformational change of gp120 and thereby block binding of HIV virion to CCR5 or CXCR4. On the other hand, BMS806 binds to gp120 and blocks the CD4 induction of the HR1 exposure without any significant effect on CD4 binding. YYA-021 also induces a highly synergistic interaction in the combinational use with the CXCR4 antagonist T140 or the neutralizing anti-V3 monoclonal antibody KD-247 and exerts a pronounced effect on the dynamic supramolecular mechanism of HIV-1 entry. CD4 mimics are essential probes directed to HIV entry, and might be important leads for the cocktail therapy of AIDS.

6. Conclusion

Since the discovery of AIDS in 1983, several inhibitory drugs against HIV replication have been developed and used clinically for treatment of patients with AIDS and HIV infection. Use of reverse transcriptase inhibitors and protease inhibitors in combination, designated HAART, has provided great success in clinical treatments. Recently, novel drugs including entry inhibitors and IN inhibitors, which belong to categories distinct from the above drugs, have been approved for clinical use. Fusion inhibitors such as Enfuvirtide, co-receptor CCR5 antagonists such as Maraviroc and IN inhibitors such as Raltegravir have successively been developed in company with the potential of other inhibitors including CXCR4 antagonists and CD4 mimics.

7. Expert opinion

In the three decades since the discovery of AIDS, the number of HIV people infected with HIV has surpassed 30 million. In the early era of the discovery of AIDS, it was thought that AIDS/HIV infectious syndrome was a lethal disease. However, with the appearance of second-generation drugs,

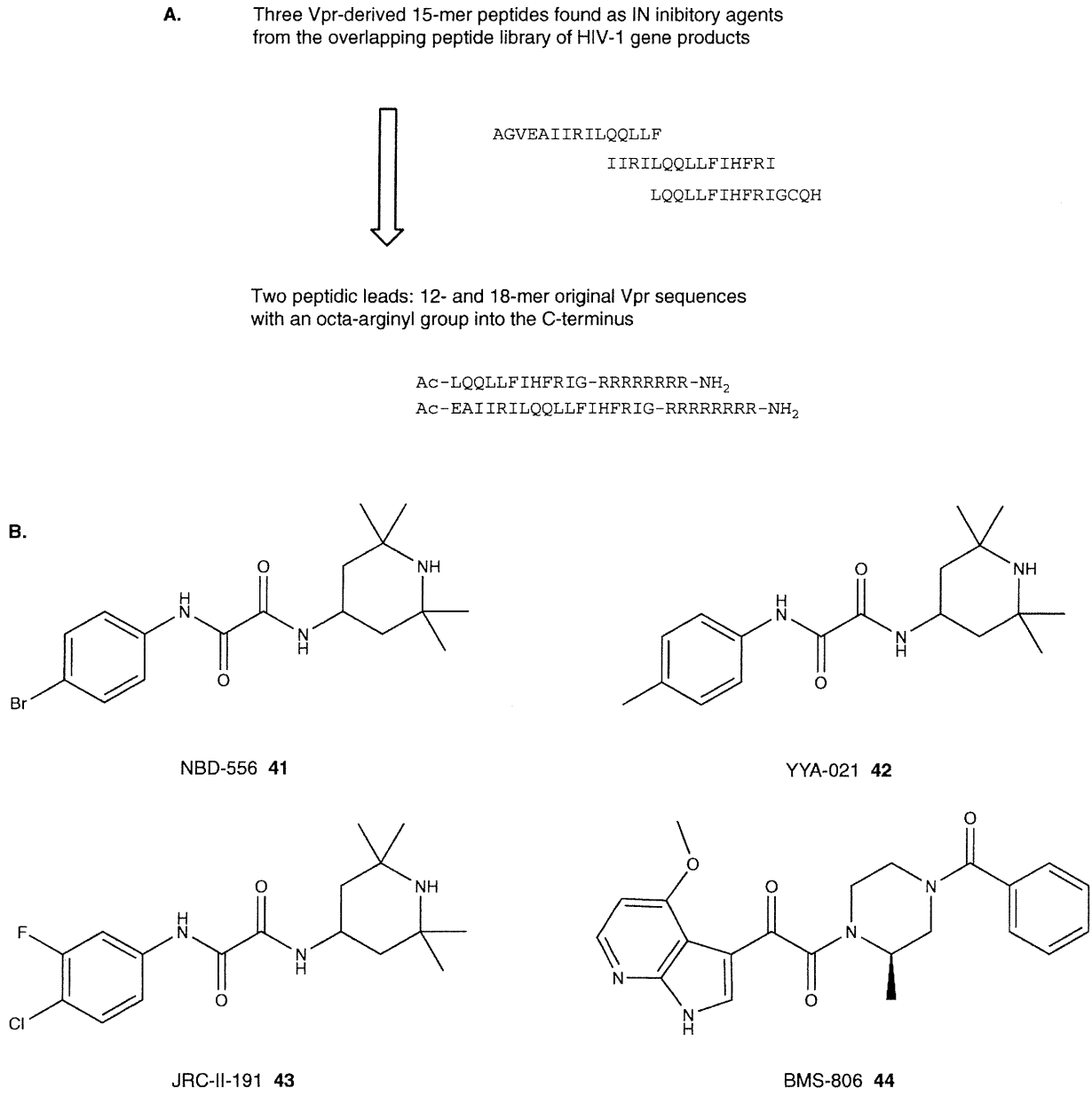

Figure 5. A. Vpr-derived IN inhibitors with an allosteric mechanism. **B.** Structures of small-sized CD4 mimics.

the protease inhibitors and introduction of a cocktail therapy (HAART), AIDS has become a curable disease. HAART can reduce the concentrations of HIV in blood to undetectable levels. There are, however, serious clinical problems including side effects, the emergence of MDR strains and high costs. Thus, brand-new drugs with novel mechanisms of action continue to be sought.

Since 1995, the molecular mechanisms underlying the HIV-1 replication have been elucidated in detail, in particular for the dynamic supramolecular mechanism associated with HIV entry/fusion steps. Elucidation of the mechanism led to the development of Enfuvirtide, which was the first entry/fusion inhibitor approved by the FDA. This drug is now used as an additional drug in the cocktail therapy for patients with evidence of HIV infection and resistance to other drugs. Enfuvirtide is not the first-choice drug, and it is not used as a monotherapy. Appearance of Enfuvirtide has an important impact in terms of its role in a repertoire of anti-HIV drugs, because it can be used even for treatment of advanced infection. Whereas reverse transcriptase inhibitors and protease inhibitors work inside of cells to inhibit functions of viral enzymes, the fusion inhibitor Enfuvirtide works extracellularly to prevent HIV from invading cells. Since fusion inhibitors are not required to penetrate cells, cell penetration is not required in drug design

and development. Entry and fusion inhibitors have this advantage. In addition, the HR1 and HR2 regions of gp41 have highly conserved sequences among various strains, without modifications of carbohydrates, suggesting that fusion inhibitors such as Enfuvirtide are likely to be able to access HIV virion of diverse strains. The HR1 region is, therefore, also critical for the development of AIDS vaccines and we have synthesized an artificial antigen molecule consisting of a novel three-helical bundle mimetic, corresponding to the trimeric form of N36. The exposed timing of its epitopes is limited during HIV-1 entry, and carbohydrates, which disturb access of antibodies to its epitopes, are not included. These two advantages could further enhance the potential of a vaccine design based on the HR1 region. Enfuvirtide and several reported C34 analogs are peptidic compounds, and development of non-peptide low molecular weight inhibitors is desirable although this is difficult and has not succeeded to date. The success of Enfuvirtide has encouraged development of entry/fusion inhibitors as a new class of anti-HIV drugs. Therefore, Maraviroc (1) was developed as the first CCR5 antagonist to be approved by the FDA. Since individuals with the CCR5-32 deletion mutation are healthy and strongly resistant to HIV-1 infection [28], it was thought that CCR5 antagonists have suitable pharmaceutical properties. Further, it might be difficult to generate resistant viruses in a use of drugs, which target host proteins such as CCR5. Accordingly, many CCR5 antagonists have been developed and some are now in clinical trials. Appearance of new CCR5 antagonists following the development of Maraviroc would be desirable. The discovery of CXCR4 has provoked vigorous research on drug development with its correlation to another co-receptor for HIV entry. However, blocking of the CXCL12–CXCR4 axis might be dangerous because CXCR4 is constitutively expressed in several organs and tissues, and CXCR4 plays a critical role in embryogenesis, homeostasis and inflammation in the fetus especially in the embryonic development of hemopoietic, cardiovascular and central nervous systems. It also plays a role in the homing of immune cells in inflammation. Knockout of CXCL12 or CXCR4 is known to be embryonically lethal [103] and thus one must carefully consider the risks associated with blockade of the CXCL12–CXCR4 axis. As anti-HIV agents, CXCR4 antagonists play a critical role in HIV-infected patients who have X4 HIV-1 strains that emerge late in the HIV infectious disease process. CXCR4 antagonists might suppress the appearance of X4 or dual-tropic strains in patients who have R5 strains that constitute a majority in the early stages of HIV infection. Combinational use of CXCR4 antagonists with CCR5 antagonists has shown potent synergism against a 1:1 mixture of X4 and R5 strains *in vitro* [104]. As anticancer agents, CXCR4 antagonists which block the CXCL12–CXCR4 interactions might represent a novel and useful chemotherapy of cancer metastasis and leukemia. CXCR4 antagonists might be useful for mobilization of hemopoietic stem cells from the bone marrow [105]. The interaction between CXCL12 and CXCR4 is correlated with the retention of stem cells in the bone marrow, and blocking this interaction results in mobilization of stem cells. AMD3100 induces not only rapid mobilization of hemopoietic stem cells [106], but also adverse cardiovascular effects. Its use as an anti-AIDS drug has been discontinued, but its development as an agent for stem cell mobilization continues [107]. In the year (2007) that Maraviroc received approval, the FDA also approved Raltegravir as the first IN inhibitor for use in combination with other antiretroviral agents in treatment-experienced patients with HIV-1 strains resistant to multiple HAART agents. Subsequently, in 2009 the FDA granted expanded approval of Raltegravir for use in combinational dosing regiments in all patients. The design of these IN inhibitors is thought to be rational since it is based on scaffold structures with a two magnesium-binding pharmacophore such as DKA, naphthyridinone and pyrimidinone-related templates. Appearance of IN inhibitors after Raltegravir for clinical use is desired. We have found Vpr-derived peptides which inhibit IN function in an allosteric manner. In future designs, these inhibitors are attractive and useful leads because the binding site is different from that used by Raltegravir. CD4 has long been a target for AIDS chemotherapy and anti-HIV drugs, and recently, several small-sized CD4 mimics have been found. Since these compounds target the dynamic supramolecular mechanism of HIV-1 entry and induce highly synergistic effects when combined with the CXCR4 antagonist T140 or the anti-V3 antibody KD-247, they might transpire to be important leads for the cocktail therapy of AIDS.

A methodology for finding of anti-HIV leads using random libraries such as overlapping peptide libraries derived from HIV-1 gene products is a useful strategy which has led to the discovery of new allosteric-type HIV IN inhibitors [94,95]. Recently, a combination therapy including an HIV protease dimerization inhibitor, Darunavir, Tibotec Pharmaceuticals, Co Cork, Ireland [108,109], and an IN inhibitor, Raltegravir, is a major first choice for drug combination regimens. In case of loss of efficacy of HAART due to the emergence of MDR strains, change of regimens of the drug combination in HAART is required with monitoring of the virus and CD4 in blood including cellular tropism testing. In such a situation, the number of available potent anti-HIV drugs is critical. Entry inhibitors such as CCR5/CXCR4 antagonists and CD4 mimics fusion inhibitors, and IN inhibitors might be optional agents for an expansion of the drug repertoire available to patients at all stages of HIV infection. Today, 20-year-old HIV-positive persons in wealthy countries starting HAART drugs can expect to live up to 69 years of age [110].

Acknowledgements

The authors wish to acknowledge their collaborators: N Fujii (Kyoto University), N Yamamoto (National University of Singapore), T Murakami (National Institute of Infectious Diseases), H Nakashima (St. Marianna University), H Mitsuya (Kumamoto University), T Hattori (Tohoku University),

M Waki (Kyushu University), A Otaka (The University of Tokushima), I Hamachi (Kyoto University), M Matsuoka (Kyoto University), S Matsushita (Kumamoto University), K Yoshimura (Kumamoto University), S Harada (Kumamoto University), JO Trent (University of Louisville), SC Peiper (Medical College of Georgia), Z Wang (Medical College of Georgia), H Xiong (University of Nebraska Medical Center), S Kusano (St. Marianna University), S Terakubo (St. Marianna University), A Ojida (Kyoto University), S Oishi (Kyoto University), S Ueda (Kyoto University), J Komano (National Institute of Infectious Diseases), E Kodama (Tohoku University), K Ohba (National University of Singapore), E Urano (National Institute of Infectious Diseases), K Maddali (National Cancer Institute), Y Pommier (National Cancer Institute), JA Beutler (National Cancer Institute), A Iwamoto (The University of Tokyo), H Tsutsumi (Tokyo Medical and Dental University), N Ohashi (Tokyo Medical and Dental University), K Hiramatsu (Kyoto University), T Araki (Kyoto University), T Ogawa (Kyoto University), H Nishikawa (Kyoto University), Y Tanabe (Tokyo Medical and Dental University), T Nakahara (Tokyo Medical and Dental University), H Arai (Tokyo Medical and Dental University), T Ozaki (Tokyo Medical and Dental University), A Sohma (Tokyo Medical and Dental University) and B Evans (Medical College of Georgia), A Omagari (Kyoto University), A Esaka (Kyoto University), M Nakamura (Kyoto University), Y Yamada (Tokyo Medical and Dental University), A Ohya (Tokyo Medical and Dental University), C Ochiai (Tokyo Medical and Dental University), A Ogawa (Tokyo Medical and Dental University) and K Itotani (Tokyo Medical and Dental University).

Declaration of interest

This work was supported in part by a Grant-in-Aid for Scientific Research from the Ministry of Education, Culture, Sports, Science and Technology, Japan; the Ministry of Health, Labour and Welfare, Japan; Japan Human Science Foundation and Health and Labour Sciences Research Grants from the Ministry of Health, Labour and Welfar, Japan. C Hashimoto and T Tanaka are grateful for the JSPS Reseach Fellowships for Young Scientist.

Bibliography

Papers of special note have been highlighted as either of interest (•) or of considerable interest (••) to readers.

1. Barre-Sinoussi F, Chermann JC, Rey F, et al. Isolation of a T-lymphotropic retrovirus from a patient at risk for acquired immune deficiency syndrome (AIDS). Science 1983;220:868-71
2. Mitsuya H, Erickson J. Drug development. A. Discovery and development of antiretroviral therapeutics for HIV infection. In: Merigan TC, Bartlett JG, Bolognesi D. editors. Textbook of AIDS Medicine. Williams & Wilkins; Baltimore; 1999. p. 751-80
3. Alkhatib G, Combadiere C, Broder CC, et al. CC CKRS: a RANTES, MIP-1alpha, MIP-1beta receptor as a fusion cofactor for macrophage-tropic HIV-1. Science 1996;272:1955-8
4. Choe H, Farzan M, Sun Y, et al. The beta-chemokine receptors CCR3 and CCR5 facilitate infection by primary HIV-1 isolates. Cell 1996;6:1135-48
5. Deng HK, Liu R, Ellmeier W, et al. Identification of a major co-receptor for primary isolates of HIV-1. Nature 1996;381:661-6
6. Doranz BJ, Rucker J, Yi YJ, et al. A dual-tropic primary HIV-1 isolate that uses fusin and the beta-chemokine receptors CKR-5, CKR-3, and CKR-2b as fusion cofactors. Cell 1996;85:1149-58
7. Dragic T, Litwin V, Allaway GP, et al. HIV-1 entry into CD4(+) cells is mediated by the chemokine receptor CC-CKR-5. Nature 1996;381:667-73
8. Feng Y, Broder CC, Kennedy PE, Berger EA. HIV-1 entry cofactor: Functional cDNA cloning of a seven-transmembrane, G protein-coupled receptor. Science 1996;272:872-7
9. Chan DC, Kim PS. HIV entry and its inhibition. Cell 1998;93:681-4
10. Wild CT, Greenwell TK, Matthews TJ, et al. A synthetic peptide from HIV-1 gp41 is a potent inhibitor of virus-mediated cell-cell fusion. AIDS Res Hum Retroviruses 1993;9:1051-3
•• **The discovery of a fusion inhibitor Enfuvirtide.**
11. Walker DK, Abel S, Comby P, et al. Species differences in the disposition of the CCR5 antagonist, UK-427,857, a new potential treatment for HIV. Drug Metab Dispos 2005;33:587-95
•• **The discovery of an entry inhibitor Maraviroc (CCR5 antagonist).**
12. Cahn P, Sued O. Raltegravir: a new antiretroviral class for salvage therapy. Lancet 2007;369:1235-6
•• **The discovery of an integrase inhibitor Raltegravir.**
13. Grinsztejn B, Nguyen B-Y, Katlama C, et al. Safety and efficacy of the HIV-1 integrase inhibitor Raltegravir (MK-0518) in treatment-experienced patients with multidrug-resistant virus: a phase II randomised controlled trial. Lancet 2007;369:1261-9
•• **The discovery of an integrase inhibitor Raltegravir.**
14. Lu M, Blacklow SC, Kim PS. A trimeric structural domain of the HIV-1 transmembrane glycoprotein. Nat Struct Biol 1995;2:1075-82
15. Shimura K, Nameki D, Kajiwara K, et al. Resistance profiles of novel electrostatically constrained HIV-1 fusion inhibitors. J Biol Chem 2010;285:39471-80
16. Chan DC, Fass D, Berger JM, Kim PS. Core structure of gp41 from the HIV envelope glycoprotein. Cell 1997;89:263-73
17. Otaka A, Nakamura M, Nameki D, et al. Remodeling of gp41-C34 peptide leads to highly effective inhibitors of the fusion of HIV-1 with target cells. Angew Chem Int Ed 2022;41:2937-40

18. Nishikawa H, Nakamura S, Kodama E, et al. Electrostatically constrained alpha-helical peptide inhibits replication of HIV-1 resistant to Enfuvirtide. Int J Biochem Cell Biol 2009;41:891-9

19. Liu S, Lu H, Xu Y, et al. Different from the HIV fusion inhibitor C34, the anti-HIV drug fuzeon (T-20) inhibits HIV-1 entry by targeting multiple sites in gp41 and gp120. J Biol Chem 2005;280:11259-73

20. Derdeyn CA, Decker JM, Sfakianos JN, et al. Sensitivity of human immunodeficiency virus type 1 to fusion inhibitors targeted to the gp41 first heptad repeat involves distinct regions of gp41 and is consistently modulated by gp120 interactions with the coreceptor. J Virol 2001;75:8605-14

21. Veiga AS, Santos NC, Loura LM, et al. HIV fusion inhibitor peptide T-1249 is able to insert or adsorb to lipidic bilayers. Putative correlation with improved efficiency. J Am Chem Soc 2004;126:14758-63

• **The discovery of a fusion inhibitor T-1249, a follow-on to Enfuvirtide.**

22. Pierson TC, Doms RW, Pohlmann S. Prospects of HIV-1 entry inhibitors as novel therapeutics. Rev Med Virol 2004;14:255-70

23. Liu S, Jiang S. High throughput screening and characterization of HIV-1 entry inhibitors targeting gp41: theories and techniques. Curr Pharm Des 2004;10:1827-43

24. Si Z, Madani N, Cox JM, et al. Small-molecule inhibitors of HIV-1 entry block receptor-induced conformational changes in the viral envelope glycoproteins. Proc Natl Acad Sci USA 2004;101:5036-41

25. Ferrer M, Kapoor TM, Strassmaier T, et al. Selection of gp41-mediated HIV-1 cell entry inhibitors from biased combinatorial libraries of non-natural binding elements. Nat Struct Biol 1999;6:953-60

26. Nakahara T, Nomura W, Ohba K, et al. Remodeling of dynamic structures of HIV-1 envelope proteins leads to synthetic antigen molecules inducing neutralizing antibodies. Bioconjug Chem 2010;21:709-14

• **The development of an HIV vaccine based on trimer mimic of the gp41 HR1 region.**

27. Zwick MB, Saphire EO, Burton DR. gp41: HIV's shy protein. Nat Med 2004;10:133-4

28. Berger EA, Murphy PM, Farber JM. Chemokine receptors as HIV-1 coreceptors: roles in viral entry, tropism, and disease. Annu Rev Immunol 1999;14:657-700

29. Abel S, Russell D, Whitlock LA, et al. Assessment of the absorption, metabolism and absolute bioavailability of Maraviroc in healthy male subjects. Br J Clin Pharmacol 2008;65:60-7

30. Chan PLS, Weatherley B, McFadyen L, et al. A population pharmacokinetic meta-analysis of Maraviroc in healthy volunteers and asymptomatic HIV-infected subjects. Br J Clin Pharmacol 2008;65:76-85

31. Stupple PA, Batchelor DV, Corless M, et al. An imidazopiperidine series of CCR5 antagonists for the treatment of HIV: The discovery of N-{(1S)-1-(3-fluorophenyl)-3-[(3-endo)-3-(5-isobutyryl-2-methyl-4,5,6,7-tetrahydro-1H-imidazo[4,5-c]pyridin-1-yl)-8-azabicyclo[3.2.1]oct-8-yl]propyl} acetamide (PF-232798). J Med Chem 2011;54:67-77

32. Baba M, Nishimura O, Kanzaki N, et al. A small-molecule, nonpeptide CCR5 antagonist with highly potent and selective anti-HIV-1 activity. Proc Natl Acad Sci USA 1999;96:5698-703

33. Shiraishi M, Aramaki Y, Seto M, et al. Discovery of novel, potent, and selective small-molecule CCR5 antagonists as anti-HIV-1 agents: Synthesis and biological evaluation of anilide derivatives with a quaternary ammonium moiety. J Med Chem 2000;43:2049-63

34. Imamura S, Ishihara Y, Hattori T, et al. CCR5 antagonists as anti-HIV-1 agents. 1. Synthesis and biological evaluation of 5-oxopyrrolidine-3-carboxamide derivatives. Chem Pharm Bull 2004;52:63-73

35. Imamura S, Ichikawa T, Nishikawa Y, et al. Discovery of a piperidine-4-carboxamide CCR5 antagonist (TAK-220) with highly potent anti-HIV-1 activity. J Med Chem 2006;49:2784-93

36. Tagat JR, McCombie SW, Nazareno DV, et al. Piperazine-based CCR5 antagonists as HIV-1 inhibitors. IV. Discovery of 1-[(4,6-dimethyl-5-pyrimidinyl)carbonyl]-4-[4-{2-methoxy-1(R)-4-(trifluoromethyl)-phenyl}ethyl-3(S)-methyl-1-piperazinyl]-4-methylpiperidine (Sch-417690/Sch-D), a potent, highly selective, and orally bioavailable CCR5 antagonists. J Med Chem 2003;47:2405-8

37. Landovitz RJ, Angel JB, Hoffmann C, et al. Phase II study of vicriviroc versus efavirenz (both with zidovudine/lamivudine) in treatment-naive subjects with HIV-1 infection. J Infect Dis 2008;198:1113-22

38. Gathe J, Diaz R, Fatkenheuer G, et al. Phase 3 trials of Vicriviroc in treatment-experienced subjects demonstrate safety but not significantly superior efficacy over potent background regimens. 17th CROI Conference on Retroviruses and Opportunistic Infections; 16 – 19 February 2010; San Francisco CA

39. Habashita H, Kokubo M, Hamano S, et al. Design, synthesis, and biological evaluation of the combinatorial library with a new spirodiketopiperazine scaffold. Discovery of novel potent and selective low-molecular-weight CCR5 antagonists. J Med Chem 2006;49:4140-52

40. Muller A, Homey B, Soto H, et al. Involvement of chemokine receptors in breast cancer metastasis. Nature 2001;410:50-6

41. Tamamura H, Hori A, Kanzaki N, et al. T140 analogs as CXCR4 antagonists identified as anti-metastatic agents in the treatment of breast cancer. FEBS Lett 2003;550:79-83

42. Takenaga M, Tamamura H, Hiramatsu K, et al. A single treatment with microcapsules containing a CXCR4 antagonist suppresses pulmonary metastasis of murine melanoma. Biochem Biophys Res Commun 2004;320:226-32

43. Tsukada N, Burger JA, Zvaifler NJ, Kipps TJ. Distinctive features of "nurselike" cells that differentiate in the

context of chronic lymphocytic leukemia. Blood 2002;99:1030-7

44. Juarez J, Bradstock KF, Gottlieb DJ, Bendall LJ. Effects of inhibitors of the chemokine receptor CXCR4 on acute lymphoblastic leukemia cells in vitro. Leukemia 2003;17:1294-300

45. Nanki T, Hayashida K, El-Gabalawy HS, et al. Stromal cell-derived factor-1-CXC chemokine receptor 4 interactions play a central role in CD4(+) T cell accumulation in rheumatoid arthritis synovium. J Immunol 2000;165:6590-8

46. Tamamura H, Fujisawa M, Hiramatsu K, et al. Identification of a CXCR4 antagonist, a T140 analog, as an anti-rheumatoid arthritis agent. FEBS Lett 2004;569:99-104

47. Tamamura H, Xu Y, Hattori T, et al. A low-molecular-weight inhibitor against the chemokine receptor CXCR4: a strong anti-HIV peptide T140. Biochem Biophys Res Commun 1998;253:877-82

- **The development of a peptidic CXCR4 antagonist T140.**

48. Tamamura H, Hiramatsu K, Kusano S, et al. Synthesis of potent CXCR4 inhibitors possessing low cytotoxicity and improved biostability based on T140 derivatives. Org Biomol Chem 2003;1:3656-62

49. Tamamura H, Hiramatsu K, Mizumoto M, et al. Enhancement of the T140-based pharmacophores leads to the development of more potent and bio-stable CXCR4 antagonists. Org Biomol Chem 2003;1:3663-9

- **The development of biostable derivatives of a CXCR4 antagonist T140.**

50. Fujii N, Oishi S, Hiramatsu K, et al. Molecular-size reduction of a potent CXCR4-chemokine antagonist using orthogonal combination of conformation- and sequence-based libraries. Angew Chem Int Ed 2003;42:3251-3

51. Schols D, Struyf S, Van Damme J, et al. Inhibition of T-tropic HIV strains by selective antagonization of the chemokine receptor CXCR4. J Exp Med 1997;186:1383-8

- **The development of a non-peptidic CXCR4 antagonist AMD3100.**

52. De Clercq E. The bicyclam AMD3100 story. Nat Rev Drug Discov 2003;2:581-7

53. Pettersson S, Perez-Nueno VI, Mena MP, et al. Novel monocyclam derivatives as HIV entry inhibitors: design, synthesis, anti-HIV evaluation, and their interaction with the CXCR4 co-receptor. ChemMedChem 2010;5:1272-81

54. Weiqiang Z, Zhongxing L, Aizhi Z, et al. Discover of small molecule CXCR4 Antagonists. J Med Chem 2007;50:5655-64

55. Zhu A, Zhan W, Liang Z, et al. Dipyridine amines: a novel class of chemokine receptor type 4 antagonists with high specificity. J Med Chem 2010;53:8556-68

56. Bridger GJ, Skerlj RT, Hernandez-Abad PE, et al. Synthesis and structure-activity relationships of azamacrocyclic C-X-C chemokine receptor 4 antagonists: analogues containing a single azamacrocyclic ring are potent inhibitors of T-cell tropic (X4) HIV-1 replication. J Med Chem 2010;53:1250-60

57. Skerlj RT, Bridger GJ, Kaller A, et al. Discovery of novel small molecule orally bioavailable C-X-C chemokine receptor 4 antagonists that are potent inhibitors of T-tropic (X4) HIV-1 replication. J Med Chem 2010;53:3376-88

58. De Clercq E. New anti-HIV agents and targets. Med Res Rev 2002;22:531-65

59. Stone ND, Dunaway SB, Flexner C, et al. Multiple-dose escalation study of the safety, pharmacokinetics, and biologic activity of oral AMD070, a selective CXCR4 receptor inhibitor, in human subjects. Antimicrob Agents Chemother 2007;51:2351-8

60. Gudmundsson KS, Sebahar PR, Richardson LD, et al. Amine substituted N-(1H-benzimidazol-2ylmethyl)-5,6,7,8-tetrahydro-8-quinolinamines as CXCR4 antagonists with potent activity against HIV-1. Bioorg Med Chem Lett 2009;19:5048-52

61. Miller JF, Turner EM, Gudmundsson KS, et al. Novel N-substituted benzimidazole CXCR4 antagonists as potential anti-HIV agents. Bioorg Med Chem Lett 2010;20:2125-8

62. Catalano JG, Gudmundsson KS, Svolto A, et al. Synthesis of a novel tricyclic 1,2,3,4,4a,5,6,10b-octahydro-1,10-phenanthroline ring system and CXCR4 antagonists with potent activity against HIV-1. Bioorg Med Chem Lett 2010;20:2186-90

63. Ueda S, Kato M, Inuki S, et al. Identification of novel non-peptide CXCR4 antagonists by ligand-based design approach. Bioorg Med Chem Lett 2008;18:4124-9

64. Tamamura H, Ojida A, Ogawa T, et al. Identification of a new class of low molecular weight antagonists against the chemokine receptor CXCR4 having the dipicolylamine-zinc(II) complex structure. J Med Chem 2006;49:3412-15

65. Tanaka T, Narumi T, Ozaki T, et al. Azamacrocyclic metal complexes as CXCR4 antagonists. ChemMedChem 2011;6:834-9

66. Ichiyama K, Yokoyama-Kumakura S, Tanaka Y, et al. A duodenally absorbable CXC chemokine receptor 4 antagonist, KRH-1636, exhibits a potent and selective anti-HIV-1 activity. Proc Natl Acad Sci USA 2003;100:4185-90

- **The development of a non-peptidic CXCR4 antagonist KRH-1636.**

67. Iwasaki Y, Akari H, Murakami T, et al. Efficient inhibition of SDF-1alpha-mediated chemotaxis and HIV-1 infection by novel CXCR4 antagonists. Cancer Sci 2009;100:778-81

68. Percherancier Y, Berchiche YA, Slight I, et al. Bioluminescence resonance energy transfer reveals ligand-induced conformational changes in CXCR4 homo- and heterodimers. J Biol Chem 2005;280:9895-903

69. Berchiche YA, Chow KY, Lagane B, et al. Direct assessment of CXCR4 mutant conformations reveals complex link between receptor structure and G(alpha)(i) activation. J Biol Chem 2007;282:5111-15

70. Tanaka T, Nomura W, Narumi T, et al. Bivalent ligands of CXCR4 with rigid linkers for elucidation of the dimerization state in cells. J Am Chem Soc 2010;132:15899-901

71. Asante-Appiah E, Skalka AM. Molecular mechanisms in retrovirus DNA integration. Antiviral Res 1997;36:139-56

72. Hindmarsh P, Leis J. Retroviral DNA integration. Microbiol Mol Biol Rev 1999;63:836-43

73. Ellison V, Brown PO. A stable complex between integrase and viral DNA ends mediates human immunodeficiency virus integration in vitro. Proc Natl Acad Sci USA 1994;91:7316-20

74. Vink C, Lutzke RAP, Plasterk RHA. Formation of a stable complex between the human immunodeficiency virus integrase protein and viral DNA. Nucleic Acids Res 1994;22:4103-10

75. Wolfe AL, Felock PJ, Hastings JC, et al. The role of manganese in promoting multimerization and assembly of human immunodeficiency virus type 1 integrase as a catalytically active complex on immobilized long terminal repeat substrates. J Virol 1996;70:1424-32

76. Grobler JA, Stillmock K, Hu B, et al. Diketo acid inhibitor mechanism and HIV-1 integrase: Implications for metal binding in the active site of phosphotransferase enzymes. Proc Natl Acad Sci USA 2002;99:6661-6

77. Hazuda DJ, Young SD, Guare JP, et al. Integrase inhibitors and cellular immunity suppress retroviral replication in rhesus macaques. Science 2004;305:528-32

78. Little S, Drusano G, Schooley R, et al. Abstract 161, 12th Conference of Retroviruses and Opportunistic Infections; Boston, MA; 2005

79. Reddy YS, Min SS, Borland J, et al. Safety and pharmacokinetics of GSK364735, a human immunodeficiency virus type 1 integrase inhibitor, following single and repeated administration in healthy adult subjects. Antimicrob Agents Chemother 2007;51:4284-9

80. Jones GS, Yu F, Zeynalzadegan A, et al. Preclinical evaluation of GS-9160, a novel inhibitor of human immunodeficiency virus type 1 integrase. Antimicrob Agents Chemother 2009;53:1194-203

81. Ferrara M, Crescenzi B, Donghi M, et al. Synthesis of a hexahydropyrimido[1,2-a]azepine-2-carboxamide derivative useful as an HIV integrase inhibitor. Tetrahedron Lett 2007;48:8379-82

82. Sato M, Motomura T, Aramaki H, et al. Novel HIV-1 integrase inhibitors derived from quinolone antibiotics. J Med Chem 2006;49:1506-8

• **The development of an integrase inhibitor Elvitegravir.**

83. DeJesus E, Berger D, Markowitz M, et al. Antiviral activity, pharmacokinetics, and dose response of the HIV-1 integrase inhibitor GS-9137 (JTK-303) in treatment-naive and treatment-experienced patients. J Acquir Immune Defic Syndr 2006;43:1-5

84. Mathias AA, German P, Murray BP, et al. Pharmacokinetics and pharmacodynamics of GS-9350: a novel pharmacokinetic enhancer without anti-HIV activity. Clin Pharmacol Ther 2010;87:322-9

85. Marinello J, Marchand C, Mott BT, et al. Comparison of Raltegravir and Elvitegravir on HIV-1 integrase catalytic reactions and on a series of drug-resistant integrase mutants. Biochemistry 2008;47:9345-54

86. Bar-Magen T, Sloan RD, Donahue DA, et al. Identification of novel mutations responsible for resistance to MK-2048, a second-generation HIV-1 integrase inhibitor. J Virol 2010;84:9210-16

• **The development of an integrase inhibitor MK-2048.**

87. Johns BA, Svolto AC. Advances in two-metal chelation inhibitors of HIV integrase. Expert Opin Ther Patents 2008;18:1225-37

88. Min S, Song I, Borland J, et al. Pharmacokinetics and safety of S/GSK1349572, a next-generation HIV integrase inhibitor, in healthy volunteers. ?Antimicrob Agents Chemother 2010;54:254-8

• **The development of an integrase inhibitor Dolutegravir.**

89. Kobayashi M, Yoshinaga T, Seki T, et al. In vitro antiretroviral properties of S/GSK1349572, a next-generation HIV integrase inhibitor. Antimicrob Agents Chemother 2011;55:813-21

90. Ovenden SP, Yu J, Wan SS, et al. Globoidnan A: a lignan from Eucalyptus globoidea inhibits HIV integrase. Phytochemistry 2004;65:3255-9

91. Valkov E, Gupta SS, Hare S, et al. Functional and structural characterization of the integrase from the prototype foamy virus. Nucleic Acids Res 2009;37:243-55

92. Hare S, Gupta SS, Valkov E, et al. Retroviral intasome assembly and inhibition of DNA strand transfer. Nature 2010;464:232-6

93. De Luca L, De Grazia S, Ferro S, et al. HIV-1 integrase strand-transfer inhibitors: design, synthesis and molecular modeling investigation. Eur J Med Chem 2011;46:756-64

94. Suzuki S, Urano E, Hashimoto C, et al. Peptide HIV-1 integrase inhibitors from HIV-1 gene products. J Med Chem 2010;53:5356-60

95. Suzuki S, Maddali K, Hashimoto C, et al. Peptidic HIV integrase inhibitors derived from HIV gene products: structure–activity relationship studies. Bioorg Med Chem 2010;18:6771-5

96. Zhao Q, Ma L, Jiang S, et al. Identification of N-phenyl-N'-(2,2,6,6-tetramethyl-piperidin-4-yl)-oxalamides as a new class of HIV-1 entry inhibitors that prevent gp120 binding to CD4. Virology 2005;339:213-25

97. Schon A, Madani N, Klein JC, et al. Thermodynamics of binding of a low-molecular-weight CD4 mimetic to HIV-1 gp120. Biochemistry 2006;45:10973-80

98. Yamada Y, Ochiai C, Yoshimura K, et al. CD4 mimics targeting the mechanism of HIV entry. Bioorg Med Chem Lett 2010;20:354-8

99. Narumi T, Ochiai C, Yoshimura K, et al. CD4 mimics targeting the HIV entry mechanism and their hybrid molecules with a CXCR4 antagonist. Bioorg Med Chem Lett 2010;20:5853-8

100. Yoshimura K, Harada S, Shibata J, et al. Enhanced exposure of human immunodeficiency virus type 1 primary isolate neutralization epitopes through binding of CD4 mimetic compounds. J Virol 2010;84:7558-68

101. Lalonde JM, Elban MA, Courter JR, et al. Design, synthesis and biological evaluation of small molecule inhibitors of CD4-gp120 binding based on virtual screening. Bioorg Med Chem 2011;19:91-101

102. Lu RJ, Tucker JA, Zinevitch T, et al. Design and synthesis of human immunodeficiency virus entry

inhibitors: sulfonamide as an isostere for the alpha-ketoamide group. J Med Chem 2007;50:6535-44

103. Zou Y-R, Kottmann AH, Kuroda M, et al. Function of the chemokine receptor CXCR4 in haematopoiesis and in cerebellar development. Nature 1998;393:595-9

104. Nakata H, Steinberg SM, Koh Y, et al. Potent synergistic anti-human immunodeficiency virus (HIV) effects using combinations of the CCR5 inhibitor aplaviroc with other anti-HIV drugs. Antimicrob Agents Chemother 2008;52:2111-19

105. Abraham M, Biyder K, Begin M, et al. Enhanced unique pattern of hematopoietic cell mobilization induced by the CXCR4 antagonist 4F-benzoyl-TN14003. Stem Cells 2007;25:2158-66

106. Broxmeyer HE, Orschell CM, Clapp DW, et al. Rapid mobilization of murine and human hematopoietic stem and progenitor cells with AMD3100, a CXCR4 antagonist. J Exp Med 2005;201:1307-18

107. Liles WC, Broxmeyer HE, Rodger E, et al. Mobilization of hematopoietic progenitor cells in healthy volunteers by AMD3100, a CXCR4 antagonist. Blood 2003;102:2728-30

108. Koh Y, Nakata H, Maeda K, et al. Novel bis-tetrahydrofuranylurethane-containing nonpeptidic protease inhibitor (PI) UIC-94017 (TMC114) with potent activity against multi-PI-resistant human immunodeficiency virus in vitro. Antimicrob Agents Chemother 2003;47:3123-9

109. Ghosh AK, Sridhar PR, Leshchenko S, et al. Structure-based design of novel HIV-1 protease inhibitors to combat drug resistance. J Med Chem 2006;49:5252-61

110. Thayer AM. This is the news from Chemical & Engineering News, American Chemical Society. p29, 2008

Affiliation

Chie Hashimoto, Tomohiro Tanaka, Tetsuo Narumi, Wataru Nomura* & Hirokazu Tamamura†
*,†Author for correspondence
Institute of Biomaterials and Bioengineering, Tokyo Medical and Dental University, Chiyoda-ku, Tokyo 101-0062, Japan
Tel: +81 3 5280 8036; Fax: +81 3 5280 8039;
E-mail: tamamura.mr@tmd.ac.jp;
E-mail: nomura.mr@tmd.ac.jp

GLIA

GLIA 59:997–1007 (2011)

HIV-1 gp120 Enhances Outward Potassium Current via CXCR4 and cAMP-Dependent Protein Kinase A Signaling in Cultured Rat Microglia

CHANGSHUI XU,[1,2] JIANUO LIU,[1] LINA CHEN,[1] SHANGDONG LIANG,[2] NOBUTAKA FUJII,[3] HIROKAZU TAMAMURA,[4] AND HUANGUI XIONG[1]*

[1]*Neurophysiology Laboratory, Department of Pharmacology and Experimental Neuroscience, University of Nebraska Medical Center, Omaha, Nebraska*

[2]*Department of Physiology, Basic Medical Institute of Nanchang University, Nanchang 330006, People's Republic of China*

[3]*Graduate School of Pharmaceutical Sciences, Kyoto University, Kyoto 606-8501, Japan*

[4]*Department of Molecular Recognition, Institute of Biomaterials and Bioengineering, Tokyo Medical and Dental University, Tokyo 101-0062, Japan*

KEY WORDS

chemokine receptors; voltage-gated K^+ channels; neuronal apoptosis; neurodegeneration

ABSTRACT

Microglia are critical cells in mediating the pathophysiology of neurodegenerative disorders such as HIV-associated neurocognitive disorders. We hypothesize that HIV-1 glycoprotein 120 (gp120) activates microglia by enhancing outward K^+ currents, resulting in microglia secretion of neurotoxins, consequent neuronal dysfunction, and death. To test this hypothesis, we studied the effects of gp120 on outward K^+ current in cultured rat microglia. Application of gp120 enhanced outward K^+ current in a dose-dependent manner, which was blocked by voltage-gated K^+ (K_v) channel blockers. Western blot analysis revealed that gp120 produced an elevated expression of K_v channel proteins. Examination of activation and inactivation of outward K^+ currents showed that gp120 shifted membrane potentials for activation and steady-state inactivation. The gp120-associated enhancement of outward K^+ current was blocked by either a CXCR4 receptor antagonist T140 or a specific protein kinase A (PKA) inhibitor H89, suggesting the involvement of chemokine receptor CXCR4 and PKA in gp120-mediated enhancement of outward K^+ current. Biological significance of gp120-induced enhancement of microglia outward K^+ current was demonstrated by experimental results showing the neurotoxic activity of gp120-stimulated microglia, evaluated by TUNEL staining and MTT assay, significantly attenuated by K_v channel blockers. Taken together, these results suggest that gp120 induces microglia neurotoxic activity by enhancing microglia outward K^+ current and that microglia K_v channels may function as a potential target for the development of therapeutic strategies.

INTRODUCTION

Microglia represent a population of resident immune cells in the brain. They are morphologically, immunophenotypically, and functionally related to cells of the monocyte/macrophage lineage and play an important role as resident immunocompetent phagocytic cells in the pathogenesis of infectious, inflammatory, and degenerative brain diseases. Upon challenging, microglia react by withdrawing their processes, becoming amoeboid and macrophage-like and undergo dramatic phenotypic, immunochemical, and functional changes, collectively referred to as "activation." The switch from resting to activation is characterized by an alteration of functional state. Resting microglia secrete neurotrophic factors, such as NGF, to support neuronal function and survival (Elkabes et al., 1998; Miwa et al., 1997). In contrast, the activated microglia produce reactive oxygen and nitrogen species and pro-inflammatory cytokines and chemokines with potential toxicity to neurons. Moreover, microglia express numerous chemokine receptors which are involved in cell migration and serve as co-receptors for HIV-1 infection. Indeed, microglia are the predominant resident CNS cell type productively infected by HIV-1 (Lipton and Gendelman, 1995). Due to poor penetration of antiviral drugs through blood-brain barrier, resident microglia (and brain macrophages) constitute a cellular reservoir of HIV-1 in the brain and a source of potential neurotoxic products (Gendelman et al., 1997; Genis et al., 1992; Koenig et al., 1986). Studies have shown that HIV-1-infected and immune-activated microglia (and brain macrophages) release a number of soluble substances including, but not limited to, pro-inflammatory cytokines, chemokines, excitatory amino acids, nitric oxide, and reactive oxygen species, as well as viral proteins, which can injure or kill neurons, contributing to the pathogenesis of HIV-1-associated neurocognitive disorders (HAND)(Garden, 2002; Kaul et al., 2001; Kielian, 2004). As such, it is imperative to identify potential target(s) for the development of therapeutic strategies to control microglia activation and/or suppress their subsequent neurotoxin production.

Increasing evidence indicates that voltage-gated K^+ (K_v) channels play a pivotal role in the process of micro-

Grant sponsor: NIH; Grant numbers: R01 NS041862-9 and 5 R01 NS063878.

*Correspondence to: Huangui Xiong, M.D., Ph.D., Department of Pharmacology and Experimental Neuroscience, University of Nebraska Medical Center, Omaha, NE 68198-5880, USA. E-mail: hxiong@unmc.edu

Received 26 May 2010; Accepted 23 February 2011

DOI 10.1002/glia.21171

Published online 24 March 2011 in Wiley Online Library (wileyonlinelibrary.com).

glia activation (Farber and Kettenmann, 2005; Walz and Bekar, 2001). Non-activated microglia express little, if any, K_v channels whereas large outward K^+ current has been observed in activated microglia (Farber and Kettenmann, 2005). Exposure to a variety of activating stimuli produces a similar pattern of electrophysiological changes in microglia. For example, lipopolysaccharide (LPS), macrophage colony-stimulating factor or interferon-γ enhances outward K^+ current in microglia (Eder et al., 1995; Fischer et al., 1995; Norenberg et al., 1994). These outward K^+ currents, which share many properties with cloned $K_v1.3$ channels, including an activation threshold at about −40 mV, strongly use-dependent inactivation, and high sensitivity to 4-aminopyridine (4-AP), agitoxin, margatoxin, and charybdotoxin (Eder et al., 1995; Fordyce et al., 2005; Norenberg et al., 1994), are predominantly recorded in activated microglia (Kotecha and Schlichter, 1999; Menteyne et al., 2009), suggesting a role for K_v channels in regulating microglia activation and cytotoxin production. It has also been shown that K_v channels expressed by activated microglia regulate their proliferation and migration (Kotecha and Schlichter, 1999; Pannasch et al., 2006). Indeed, activated microglia injure neurons, and a blockade of microglia K_v channels inhibits microglia-induced neurotoxicity (Fordyce et al., 2005). These findings stimulate our hypothesis that HIV-1 infection activates microglia by enhancing outward K^+ currents, resulting in microglia production of neurotoxins and consequent neuronal dysfunction and injury. In this study, we tested our hypothesis by exploring the effects of HIV-1 glycoprotein 120 (gp120) on outward K^+ current recorded in cultured rat microglia. Our results showed that gp120 enhanced microglia outward K^+ current via CXCR4 and cAMP-dependent protein kinase A (PKA) signaling pathway, leading to microglia production of neurotoxins and resultant neuronal apoptosis.

MATERIALS AND METHODS

Materials

HIV-1gp120 IIIB was purchased from Immunodiagnostics (Woburn, MA). Aliquots of gp120 were kept as 100 nM stock solution at −80°C. The stock solution was diluted to desired concentrations with artificial cerebrospinal fluid (ACSF) 2–5 min before tests. T140 was kindly provided by Professor Nobutaka Fujii (Kyoto, Japan). All chemicals, unless otherwise specified, were from Sigma (St. Louis, MO).

Isolation and Culture of Microglia and Cortical Neurons

Microglia and cortical neuronal cultures were obtained from the cerebral cortices of 1–2 days old or embryonic (E18) Sprague-Dawley rats (Charles River Laboratories, Wilmington, MA). Briefly, the pups were anesthetized hypothermically and decapitated, and cerebral cortices were dissected out. The cortical tissues were enzymatically digested followed by mechanical dissociation. The mixed primary cultures were grown on 75 cm^2 flasks in 30 mL (10^6 cells/mL) DMEM supplemented with 10% FBS, 2 mM glutamine, and 1% PEN/Strep (37°C, 5%CO_2). After 7–10 days in culture, microglial cells were harvested by gentle shaking, and then plated on uncoated 35 mm plastic Petri dishes at a density of 0.5 × 10^6 cells per dish. Non-adhering cells were removed 30 min after plating by changing the medium. The purity of resulting culture was judged by staining with OX-42 antibody (a marker for the microglia CR3/CD11b receptor). Cells were utilized for whole-cell recording 2 days after plating. In all cases, the culture medium was replaced with fresh ACSF on experimental day. Experiments were conducted 1–2 h after treatment with the reagents. Controls were performed in untreated and age-matched microglial cultures. For cortical neuronal cultures, the cells were plated in poly-D-lysine coated 24 well plates containing 1 mL of medium, with a cell density of 1.0 × 10^5/mL. The cultures were maintained in neurobasal medium supplemented with 1% penicillin/streptomycin, B27(2%, v/v, Invitrogen, San Diego, CA), and L-glutamine (0.5 mM) for at least 7–10 days before being used for experiments. All animal use procedures were strictly reviewed by the Institutional Animal Care and Use Committee (IACUC) of the University of Nebraska Medical Center (IACUC No. 00-062-07).

Electrophysiology

Whole-cell outward K^+ currents were recorded from cultured microglia using an Axopatch 200B amplifier. After establishment of the whole-cell configuration, the cells were allowed to stabilize for 3–5 min before recording. The recorded cells were voltage-clamped at −60 mV and whole-cell outward K^+ current was induced by voltage steps from the holding potential of −60 to −40 mV in the first step, then stepped to +60 mV in increments of 10 mV. The ACSF contained (in mM): 140 NaCl, 5 KCl, 2.0 $CoCl_2$, 1 $MgCl_2$, 10 D-glucose, 10 HEPES (pH 7.4 adjusted with NaOH, osmolarity: 310 mOsm). The recording electrodes were made from borosilcate glass capillaries and had resistance of 5–7.5 MΩ when filled with an intracellular solution contained (in mM): 135 K-gluconate, 10 KCl, 1 $CaCl_2$, 1 $MgCl_2$, 10 EGTA, 0.5 Tris-GTP, 2 Mg-ATP,10 HEPES (Adjusted pH to 7.3 with KOH, osmolarity: 300 mOsm). The seal resistance was 1–10 GΩ. Junction potentials were corrected and the cell capacitance was compensated (~ 70%) in most cells. Current signals were filtered at 1 kHz and digitized at 5 kHz using a Digidata 1440A digitizer. The current and voltage traces were displayed and recorded in a Dell computer using pCLAMP 10 data acquisition/analysis system.

The activation was studied by measuring the peak K^+ conductance (G) during a 700 ms test pulse by varying test potentials from a holding potential of −60 mV. G was calculated starting from $G = I_{peak}/V$, where I_{peak} is the peak outward K^+ current during the test potential (V). Data were normalized to maximum peak conductance (G_{max}) and fitted to Boltzmann equation: G/G_{max} =

$1/[1 + \exp(V - V_{1/2})/k]$, where $V_{1/2}$ is the voltage for half maximal activation, and k is the slope constant (mV). To study steady-state inactivation, cells were held at prepulse potentials ranging from −80 to +10 mV for 60 s and then subject to a +20 mV test pulse for 200 ms. Normalized steady-state currents were plotted versus prepulse potentials, and the curves were fitted by the Boltzmann function: $I/I_{max} = 1/[1 + \exp(V_{pp} - V_{1/2})/k]$, where I_{max} is the maximum current, $V_{1/2}$ is the voltage for half maximal activation, and V_{pp} is the voltage of the prepulse potential.

Immunocytochemistry

Immunocytochemistry was performed to substantiate the capacity of gp120 enhancing expression of microglia K_v channel, particularly $K_v1.3$. Microglia were platted on poly-D-lysine coated coverslips at a density of 0.5×10^6 cells per well in 24 well plates. Twenty-four hour later, microglia were activated by gp120 with or without tetraethylammonium (TEA, 5 mM) or 4-AP (1 mM). After another 24 h, the microglia were washed in PBS three times, fixed with 4% paraformaldehyde (PFA) for 30 min at room temperature. After washing, the microglia were blocked and permeabilized in PBS containing 10% normal goat serum, 0.2% Triton X-100, and 0.1M glycine for 30 min. Primary antibodies, including rat polyclonal antibody Mac-1 (CD11b; 1/500; Serotec) and rabbit polyclonal antibody to $K_v1.3$ (Almonade Lab, Israel), were diluted in PBS with 10% goat serum and applied to coverslips for 1 h. After washing in PBS (5 min, 3 times) Alexa Fluor 488 and Alexa Fluor 594-conjugated secondary antibodies were added for 1 h. Coverslips were mounted on slides with ProLong Gold antifade reagent +DAPI (Molecular Probes), and images were taken with a 40× oil-immersion objective.

Microglia and Neuronal Co-Culture and TUNEL Assay

TUNEL assay was performed using the *in situ* cell death detection kit, AP (Roche Applied Science, Indianapolis, IN). Rat microglia were seeded on transwell inserts (0.5×10^6 cells per well) in 24 well plates and left untreated or exposed to LPS (0.5 μg/mL, as a positive control), gp120 or gp120 plus 4-AP/TEA/H89/T140. Twenty-four hour later, microglia were washed and co-cultured with cortical neurons growing on poly-D-lysine coated coverslips at a density of 1.0×10^5 cells/well in 24-well plates for 24 h. The cortical neurons were then washed in PBS (5 min, 3 times) and fixed with 4% PFA in PBS (pH 7.4) for 1 h at room temperature. After washing three times with PBS, neurons were permeabilized with 0.1% Triton X-100 in 0.1% sodium citrate for 2 min on ice and then washed in PBS (5 min, 3 times). The neurons were then incubated with TUNEL reaction mixture that consisting of terminal deoxynucleotide transferase and fluorescein-labeled nucleotides for incorporation into DNA strand breaks at 37°C. After a final wash in PBS (5 min, 3 times), coverslips were mounted in ProLong Gold antifade reagent with DAPI (Molecular Probes, Eugene, OR). Cells were visualized by Zeiss LSM 510 META NLO microscope an a 40× oil-immersion objective. TUNEL positive cells were counted and expressed as a percentage of total number of cells counted.

MTT Assay

The assay is based on the ability of active mitochondrial dehydrogenase to convert dissolved MTT to water-insoluble purple formazan crystals. Neurons washed in PBS (5 min, 3 times) were incubated with fresh neuronal culture media containing MTT (500 μg/mL) for 3 h. At the end of incubation, the MTT solution was replaced with 500 μL of dimethyl sulfoxide (DMSO) for cell lysis. The plate was shaken for 10 min to solubilize the formazan crystals, and the optical density (OD) at 570 nm was measured.

Statistical Analysis

Experimental data were expressed as mean ± SEM. Statistical analyses were performed by ANOVA or Student t tests. A minimum P value of 0.05 was estimated as the significance level for all tests.

RESULTS

Expression of K_v Channels in Microglia

In seeking to determine whether K_v channels regulate microglia activation, we first examined K_v channel expression in rat microglia by recording the whole-cell outward K^+ current induced by voltage steps (see Fig. 1). In one group of microglia cultures ($n = 9$), the average instantaneous outward K^+ current (an A-type-like outward current) density was 79.8 ± 6.3 pA/pF, and it was reduced to 46.7 ± 5.5 pA/pF when 4-AP was added to the bath. In another group of microglial cells ($n = 9$), the average steady-state K^+ current was 46.8 ± 10.4 pA/pF, and it was reduced to 33.9 ± 9.2 pA/pF when 5 mM TEA was introduced to the bath. Addition of 4-AP or TEA to the bath produced 41.5 ± 7.2% or 27.6 ± 8.9% reduction of outward K^+ current, respectively (see Fig. 1). To estimate K^+ current density, the capacitance of microglial cells was determined and used to obtain an estimate of cell surface area. The average whole-cell capacitance was 12.4 ± 3.0 pF, with a range of 5–27.5 pF ($n = 75$).

Enhancement of Microglia Outward K^+ Current by gp120

Following confirmation of K_v channel expression in microglia, we tested if gp120 could alter the outward K^+ current in microglia. Incubation of microglia with gp120 for 1–2 h enhanced whole cell outward K^+ current in a dose-dependent manner (see Fig. 2). When microglia were treated with gp120 at concentrations of 100, 200, and 400 pM, the average instantaneous outward K^+ cur-

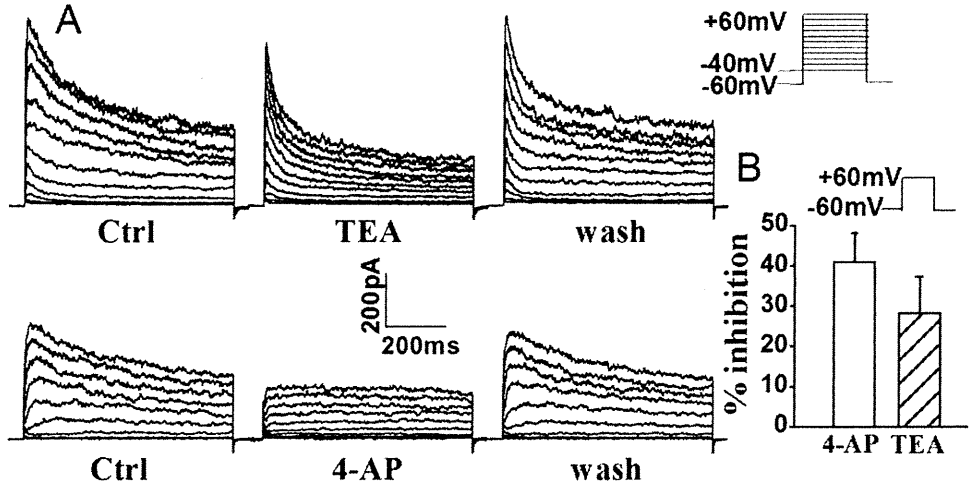

Fig. 1. Expression of outward K^+ current in rat microglia. Panel A shows examples illustrating the voltage-dependent outward K^+ current recorded in rat microglia and the partial blockade of outward K^+ current by TEA (upper) and 4-AP (lower). Panel B depicts the average inhibition of whole-cell outward K^+ current in microglia by 4-AP and TEA when measured at command voltage step of +60 mV. Bars represent mean ± SEM (the same in the following figures unless indicated). Voltage protocol employed to generate outward K^+ current is shown above Panel B.

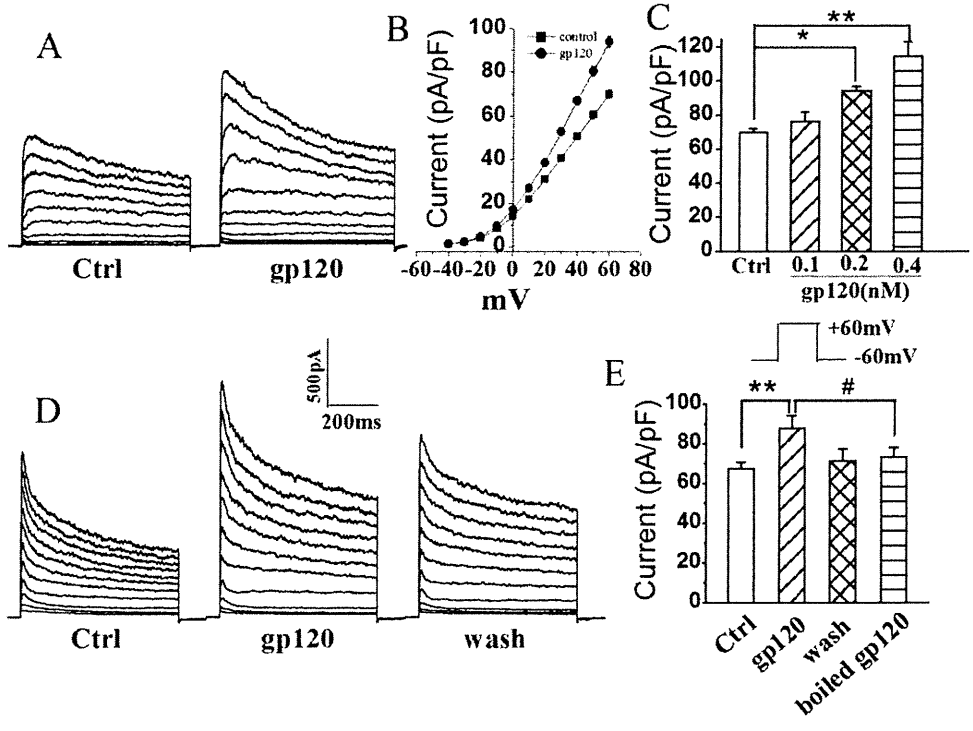

Fig. 2. gp120 enhances microglia whole-cell outward K^+ current in a dose-dependent manner. **A**: Typical outward K^+ currents recorded from a control and a gp120-treated microglia as indicated. **B**: I–V curves showing gp120 increases outward K^+ current. **C**: gp120 increases outward K^+ current in a dose-dependent manner. The graph plots mean outward K^+ current densities measured at +60 mV. **D**: Outward K^+ current recorded in microglia before (Ctrl), during (gp120), and after (wash) bath application of gp120 (200 pM). **E**: Average outward K^+ current densities recorded in microglia cells as shown in **D** (n = 5) and in another five microglia treated with heat (boiled)-inactivated gp120, illustrating gp120 specific enhancement of outward K^+ current. *, $P < 0.05$ vs. Ctrl; **, $P < 0.01$ vs. Ctrl; #, $P < 0.05$ vs. boiled gp120.

rent densities (pA/pF) were 76.1 ± 5.7 (n = 27), 94.0 ± 2.6 (n = 67), and 114.5 ± 8.4 (n = 11), respectively (see Fig. 2). In comparison with the average outward K^+ current density of 69.8 ± 2.1 pA/pF recorded in untreated (control) microglia (n = 46), the differences were statistically significant ($P < 0.05$), demonstrating an enhancement of whole cell outward K^+ current by gp120 in cultured rat microglia. Incubation of microglia with heat (boiled)-inactivated gp120 (200 pM) showed no significant effect on outward K^+ current density with an average of 73.3 ± 4.7 pA/pF (Fig. 2; n = 5), indicating a specific effect of gp120 on enhancing outward K^+ current in microglia.

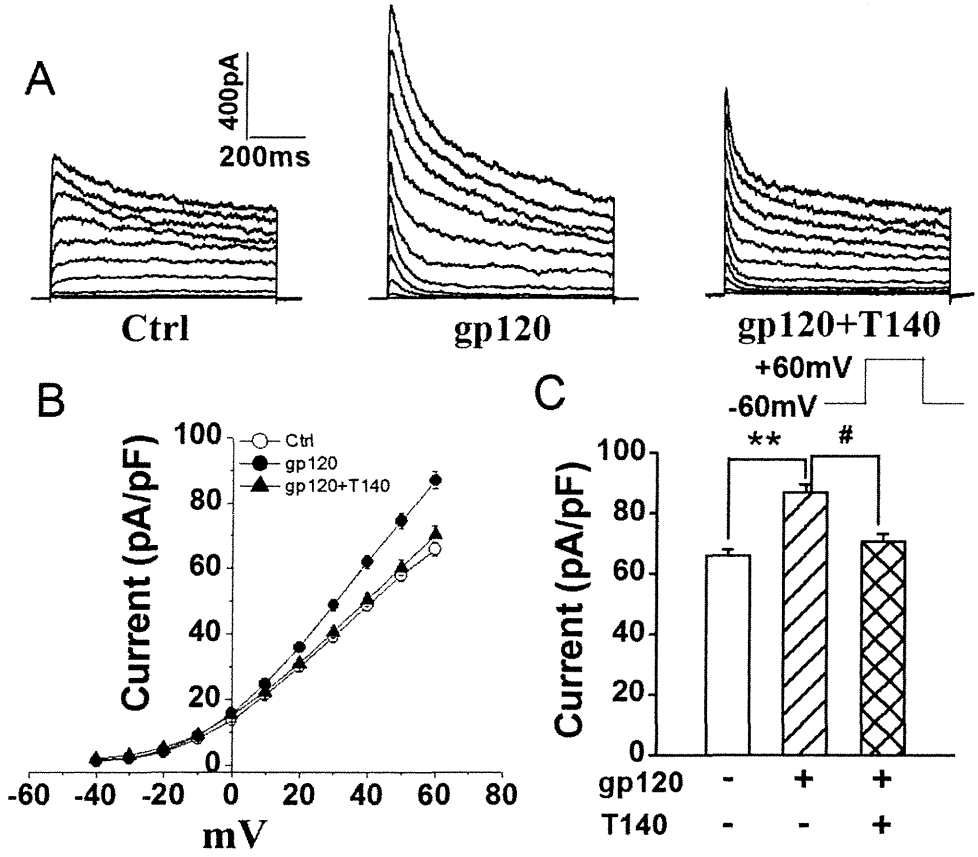

Fig. 3. Blockade of gp120-induced enhancement of microglial outward K^+ current by T140, a specific CXCR4 antagonist. **A**: Typical current traces recorded from control, gp120−, and gp120+T140-treated microglia as indicated. **B**: I–V curves of peak outward K^+ currents as shown in A. **C**: Bar graph showing the mean current densities (measured at +60 mV) recorded in control, gp120−, and gp120+T140-treated microglia. Note that gp120 enhanced outward K+ current and this enhancement was blocked by T140. ** $P < 0.01$ vs. ctrl; # $P < 0.05$ vs. gp120+T140.

Blockade of gp120-Induced Enhancement of Outward K^+ Current by T140

It is well-known that microglia express chemokine receptor CXCR4 (Albright et al., 1999; Lavi et al., 1997). To examine if the gp120-induced enhancement of outward K^+ current was mediated through CXCR4 (a co-receptor for HIV-1 infection), we tested the effects of T140, a highly selective CXCR4 receptor antagonist, on gp120-induced enhancement of outward K^+ current in another group of cultured microglia. While it *per se* had no significant effect on outward K^+ current when added to the bath, T140 (50 nM) significantly blocked gp120-induced enhancement of outward K^+ current recorded in microglia. The average instantaneous K^+ current densities without (control) and with addition of gp120 (200 pM) to the bath solution were 65.9 ± 2.2 pA/pF (n = 92) and 86.9 ± 2.7 pA/pF (n = 75), respectively. In contrast, the current density was 70.6 ± 2.5 pA/pF (n = 64) when both T140 and gp120 were added to the bath. In comparison with the K^+ current recorded when gp120 was added alone, the difference was statistically significant ($P < 0.05$), indicating that gp120 increases microglia outward K^+ current via CXCR4 (Fig. 3A,B).

Effect of gp120 on Microglia K_v Channel Biophysical Properties

To determine if gp120 alters microglia K_v channel biophysical properties, we examined the influence of gp120 on the properties of microglia K_v channel activation and steady-state inactivation. Figure 4A illustrates superimposed currents elicited by voltage steps applied in 10 mV increments from the holding potential −60 to +60 mV. Outward K^+ currents were first seen at −40 mV in gp120-treated microglia and became larger at stronger depolarizing command voltages. Normalized outward K^+ currents (Fig. 4A) were fitted to a Boltzmann equation: $G/G_{max} = 1/[1 + \exp(V - V_{1/2})/k]$, from which the voltage for half-maximal activation ($V_{1/2}$) and the slope factor (k) were calculated (Fig. 4C). Half-maximal activation occurred at 8.3 ± 0.9 mV and 12.9 ± 0.9 mV, with a slope factor, k, of 16.8 ± 0.9 mV and 15.2 ± 0.8mV for gp120-treated and control microglia, respectively (Fig. 4C; n = 21). The steady-state voltage dependence of inactivation of K^+ current was generated by varying the holding potential between −80 and +10 mV in 10 mV increments (Fig. 4B). After the holding potential was established for at least 1 min, cells

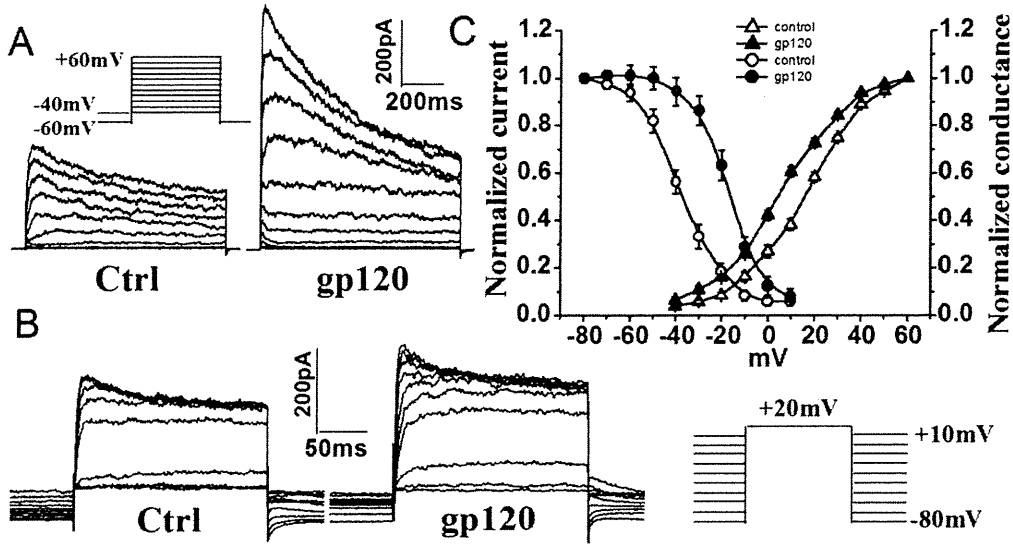

Fig. 4. Effects of gp120 on activation and inactivation of outward K^+ currents. **A**: Activation of outward K^+ current was induced using 700 ms voltage steps from a holding potential of −60 mV–40 mV at the first step, and then step to +60 mV in 10 mV increments. To ensure complete recovery from inactivation, successive voltage steps were separated by 5 s. **B**: Steady-state inactivation was measured by varying the holding potential (−80 – +10 mV) for 60 s at each voltage, then applying a 200 ms test pulse to +20 mV. **C**: Average of activation and inactivation curves. Note that gp120 shifted activation and inactivation to more negative potential and more negative potential, respectively.

were pulsed to a test potential of 20 mV for 200 ms. Steady-state inactivation began at approximately −70 mV and was complete at ~ 0 mV. Peak amplitudes of the evoked currents were measured, normalized, and then plotted as a function of the holding potential (Fig. 4B,C). The region under the intersection of activation and inactivation illustrates a window of tonic channel activity between −35 and 10 mV with maximal activity at the intersection voltage of −10 mV. Fitted with a Boltzmann function, half-maximal inactivation was at −15.4 ± 0.7 mV and −36.3 ± 0.8 mV, with k = 9.1 ± 0.7 mV and 10.1 ± 0.7 mV (n = 14) in gp120-treated and control microglia, respectively. In all cases, the voltage-dependent currents were highly K^+ selective because the reversal potential was very close to the calculated Nernst potential (−85 mV, data not shown) for K^+ concentrations used in this study (see Materials and Methods).

Involvement of PKA in gp120-Induced Increase of Outward K^+ Current

Protein phosphorylation can profoundly influence ion channel activity. Accumulating evidence indicate that K_v channels can be regulated by c-AMP-dependent protein kinase (PKA) (Chung and Schlichter, 1997; Fakler et al., 1994). We hypothesize that gp120 increases outward K^+ current via CXCR4 → PKA → K_v channel pathway. To test this hypothesis, we examined the effects of H89 (400 nM) on gp120 (200 pM)-induced enhancement of outward K^+ current in rat microglia. When applied alone, H89 failed to inhibit outward K^+ current (n = 28). In contrast, when co-applied with gp120, H89 inhibited the gp120-associated increase of outward K^+ current (see Fig. 5). The average outward K^+ current before (gp120) and after co-application of H89+gp120 were 86.2 ± 2.7 pA/pF (n = 75) and 69.1 ± 1.8 pA/pF (n = 42), respectively. The difference was statistically significant ($P < 0.05$), suggesting the involvement of PKA in gp120-induced increase of outward K^+ current.

Blockade of Microglia K_v Channels Inhibited Microglia-Induced Neuronal Injury

To examine biological significance of gp120-associated enhancement of outward K+ current, we studied neurotoxic activity of gp120-stimulated microglia and the protective effects of K_v channel blockers on microglia-induced neuronal injury. Rat microglia grown on the transwells were exposed to gp120 (200–500 pM) with or without K_v channel blockers (4-AP, 1 mM or TEA, 5 mM) for 24 h. After washing, the rat microglia were co-cultured with rat cortical neurons for additional 24 h and results showed that gp120-stimulated microglia induced apoptosis in 33.2 ± 3.9% of neurons examined (Fig. 6A,B). In comparison with the results of 4.7 ± 1.7% obtained in neurons co-cultured with non-stimulated microglia (control), the difference is statistically significant ($P < 0.01$), suggesting that gp120-stimulated microglia injure neurons. The injurious effect of microglia on neurons was confirmed by MTT assay (Fig. 6C). The neurotoxic effects of gp120-stimulated microglia were attenuated by K_v channel blockers (4-AP, TEA), CXCR4 receptor antagonist (T140), and PKA inhibitor (H89), respectively (see Fig. 6). As a positive control, LPS (0.5 μg/mL) was tested to stimulate microglia and the LPS-stimulated microglia, as anticipated, produced

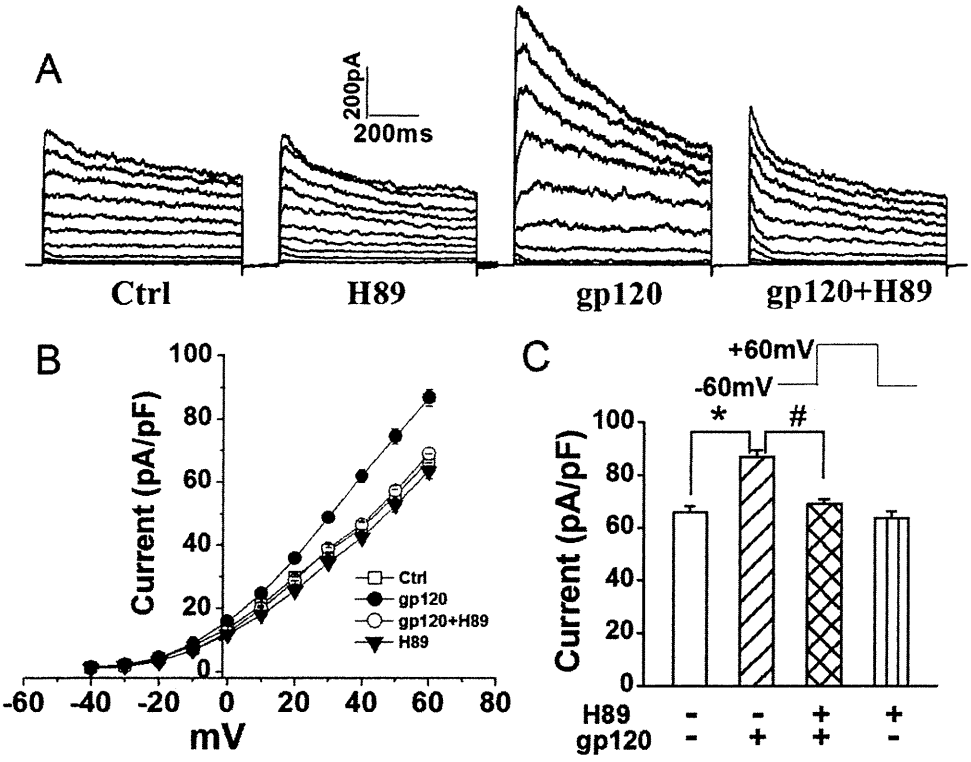

Fig. 5. Blockade of gp120-induced enhancement of outward K^+ currents by H89, a specific inhibitor for PKA. **A**: Representative current traces recorded from a control cell (Ctrl) and cells treated respectively with H89 alone, gp120 alone, and gp120+H89. The voltage protocol used to generate outward K^+ current was the same as the one shown in Fig. 1. **B**: I–V relationship illustrating the outward K^+ current densities as a function of voltage from the current traces shown in A. **C**: Summarized bar graphs showing average outward K^+ current densities measured at a voltage step +60 mV from microglia treated with H89 alone, gp120 alone, and gp120+H89. Note a significant blockade of gp120 enhancement of outward K^+ currents recorded in microglia. * $P < 0.05$ vs. ctrl, # $P < 0.05$ vs. gp120.

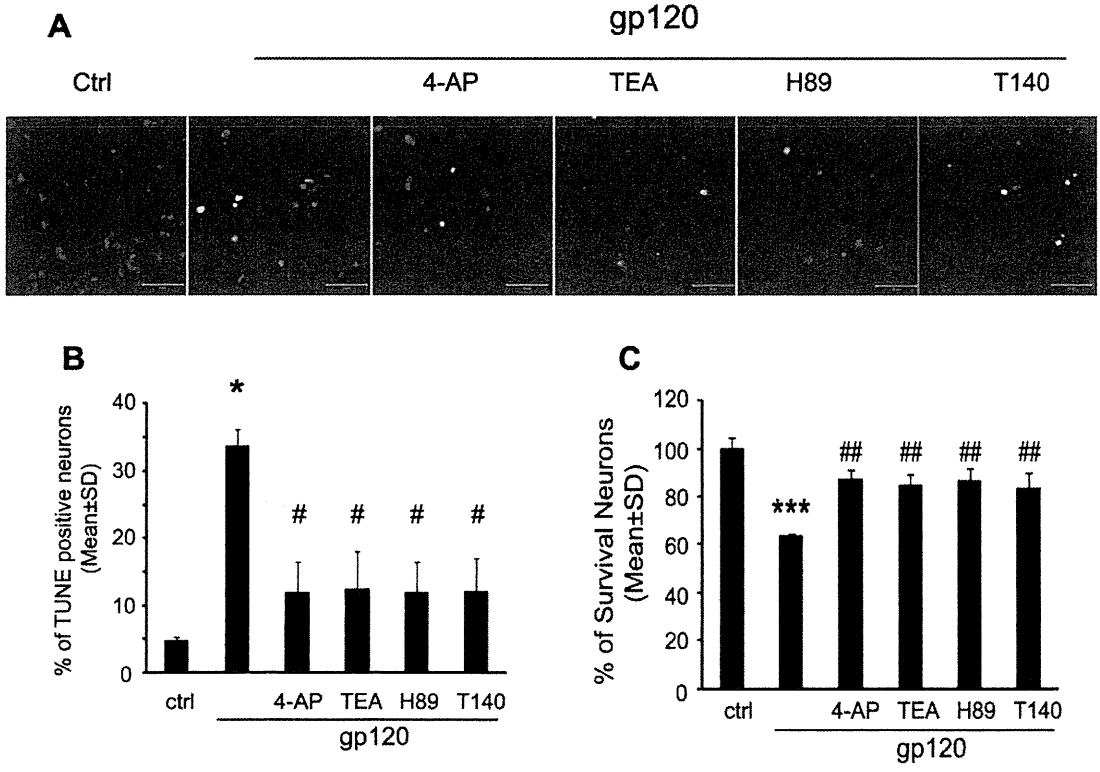

Fig. 6. Gp120-activated microglia produced cytotoxicity on neurons. Panel A: apoptotic neurons were visualized by TUNEL staining at ×400 original magnification (scale bar 50 μm). Panel B: Neuronal apoptosis was analyzed by combined TUNEL/DAPI staining and percentage of apoptotic neurons was determined by TUNEL-positive cells to normalize the total number of DAPI-positive cells. Compared with control group, an increasing percentage of apoptotic neurons were notably observed in gp120 treated group (Control vs. gp120, 7.7% vs. 33.77%). The apoptosis induced by gp120-stimulated microglia were attenuated by 4-AP, TEA, H89, and T140. Panel C: Neuronal viability was assessed by MTT assay. 4-AP, TEA, H89, and T140 significantly attenuated the neurotoxic activity of gp120-stimulated microglia. Values are expressed as mean ± SD of triplicate cultures. The results are representative of three independent experiments performed in triplicate determinations. *$P < 0.05$, ***$P < 0.001$ vs. Ctrl, # $P < 0.05$, ## $P < 0.01$ vs. gp120.

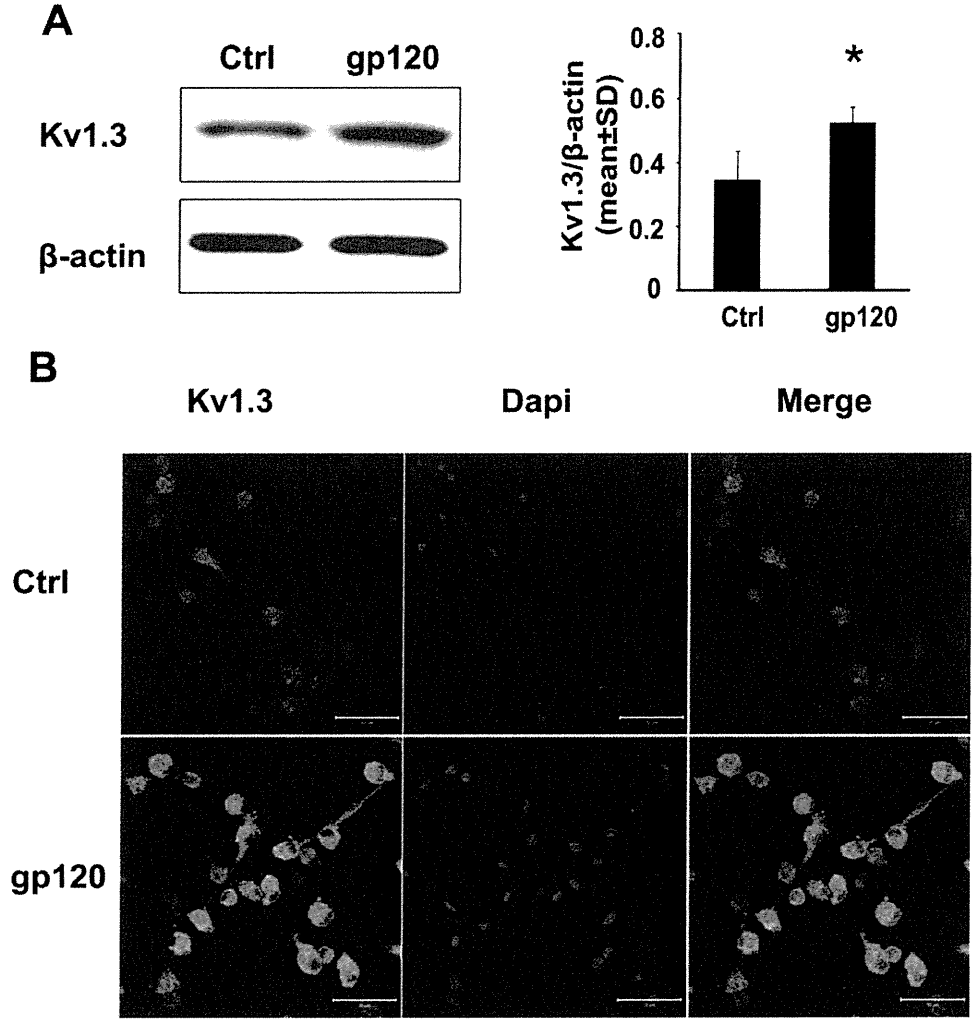

Fig. 7. gp120 enhanced expression levels of $K_v1.3$ in cultured microglia. Rat microglia (2×10^6 cells/well in 6 well plates or 0.5×10^6 cells/well in 24 well plates) were treated with or without gp120 (500 pM) for 24 h. The expression levels of $K_v1.3$ channel proteins were examined by Western blot and immunocytochemistry. Panel A: the representative scans showed Western blots for $K_v1.3$, and internal control β-actin (left). Each band density was normalized to its internal control and represents in bar graphs (right). Significant differences were detected in gp120 (1.5-fold increase) compared with nontreated microglia. $^*P < 0.05$ in comparison to control group were analyzed using Student's *t*-test. Panel B: Microglia were immunostained for expression of $K_v1.3$ (green). Images were visualized by fluorescent confocal microscopy at ×400 original magnification (scale bar 50 μm).

a significant neuronal apoptosis when co-cultured with neurons (data not shown).

Effects of gp120 on Microglia K_v Channel Expression

The voltage dependence of activation and inactivation of the outward K^+ current recorded in rat microglia, plus its blockade by 4-AP and TEA, suggest a possible identity of $K_v1.3$ current, which is in agreement with the up-regulated expression levels of $K_v1.3$ mRNA observed by other investigators (Eder, 1998; Norenberg et al., 1994; Schilling et al., 2000). To assess whether gp120 alters $K_v1.3$ protein expression, we examined the expression levels of $K_v1.3$ protein in microglia (2×10^6 cells/well, in six well plates) treated with or without gp120 for 24 h by western blot and immunocytochemistry. Our results showed that gp120 enhanced both the expression levels of $K_v1.3$ channel protein and immunofluorescent density of $K_v1.3$ staining in cultured microglia (see Fig. 7). The increase of $K_v1.3$ channel expression following gp120 treatment may underlie gp120-associated enhancement of outward K^+ current recorded in rat microglia.

Specific $K_v1.3$ Antagonist Blocks gp120-Induced Increase of Outward K^+ Current and Neuronal Apoptosis

After demonstration of gp120 enhancement of $K_v1.3$ expression, we further verified if the newly formed channels were functionally active and involved in gp120-associated increase of outward K^+ current and neuronal apoptosis using a specific $K_v1.3$ blocker margatoxin, MgTx, (Knaus et al., 1995). In another group of experiments, incubation of microglia with gp120 produced a signifi-

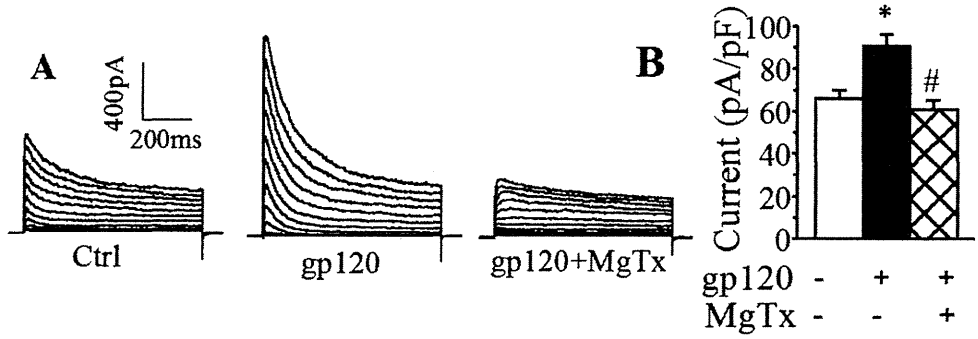

Fig. 8. Blockade of gp120 enhancement of outward K^+ current by MgTx, a specific $K_v1.3$ blocker. **A**: An example showing blockade of gp120-induced enhancement of outward K^+ current in rat microglia by MgTx. **B**: A summary bar graph illustrating MgTx significantly blocked gp120-induced enhancement of microglia outward K^+ current. Instantaneous outward K^+ current generated by a voltage step from −60 to +60 mV were measured and current densities were calculated. *, $P <$ 0.01 gp120-MgTx- vs. gp120+MgTx-; #, $P <$ 0.01 gp120+MgTx- vs. gp120+MgTx+.

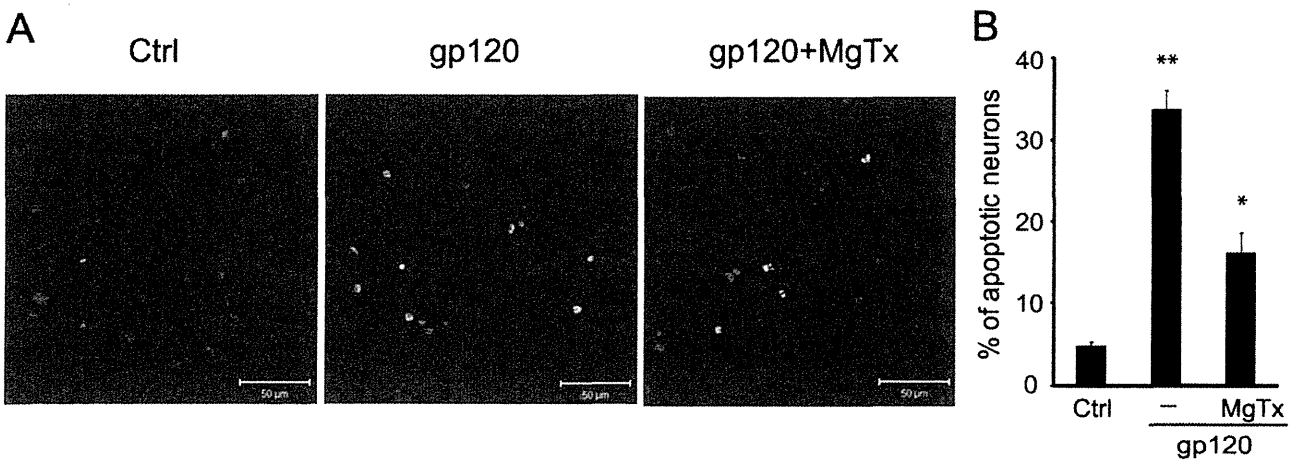

Fig. 9. Neurotoxic activity induced by gp120-stimulated microglia was blocked by MgTx in a microglia-neuronal co-culture system. **A**: Apoptotic neurons were assayed by TUNEL staining and visualized (green) via confocal microscopy at ×400 original magnifications. Scale bar equals 50 μM. **B**: Quantification of apoptotic neurons was made by enumeration of TUNEL-positive cells and expressed as percentage of total number of DAPI-positive cells counted. Note that gp120-stimulated microglia produced a significant increase of apoptotic neurons and the blockade of microglia $K_v1.3$ channel by MgTx significantly reduced microglia-induced neuronal apoptosis.

cant ($P < 0.01$) enhancement of outward K^+ current with an average current density of 90.4 ± 5.7 pA/pF (Fig. 8; $n = 12$) when compared with the current density (65.7 ± 4.3 pA/pF, $n = 10$) recorded in control (without gp120 treatment) microglia. Addition of MgTx (100 nM) to the bath solution abolished gp120-induced increase of outward K^+ current with an average of instantaneous current density of 60.5 ± 4.5 pA/pF (Fig. 8; $n = 8$). In comparison with the current density recorded in microglia treated with gp120, the difference was statistically significant ($P < 0.01$). The involvement of $K_v1.3$ in gp120-innduced neuronal injury was demonstrated by the results showing a significant attenuation of gp120-induced neuronal apoptosis by pretreatment of microglia with MgTx in microglia-neuronal co-culture system as shown in Fig. 9. These results indicate that the newly formed $K_v1.3$ channels were functional and involved in gp120-associated enhancement of outward K^+ current in rat microglia.

DISCUSSION

As the targets for HIV-1 infection and the producers of neurotoxins, microglia play an important role in the pathogenesis of HAND and other neurodegenerative disorders. It is widely accepted that the infected and immune-activated microglia secrete a variety of bioactive substances including viral protein gp120, resulting in neuronal dysfunction and death (Garden, 2002; Glass and Wesselingh, 2001). The mechanisms underlying microglia-associated neuropathogenesis are not fully understood. In this study, we demonstrated that HIV-1 gp120 increased the levels of $K_v1.3$ expression and enhanced outward K^+ current in cultured rat microglia via CXCR4-PKA signaling pathways. The enhancement of outward K^+ current was associated with microglia neurotoxicity evident through experimental results showing the blockade of microglia $K_v1.3$ channels suppressed microglia-associated neurotoxicity *in vitro*.